

2Q

DOCUMENT RESUME

ED 195 411

SE 033 402

AUTHOR Reihman, Thomas C.
 TITLE Nuclear Engineering Computer Modules,
 Thermal-Hydraulics, TH-2: Liquid Metal Fast Breeder
 Reactors.
 INSTITUTION Virginia Polytechnic Inst. and State Univ.,
 Blacksburg. Coll. of Engineering.
 SPONS AGENCY National Science Foundation, Washington, D.C.
 PUB DATE [73]
 GPANT NSF-GZ-2888: NSF-SED73-06276
 NOTE 93p.: For related documents, see SE 033 401-403.
 Contains marginal legibility in computer
 printouts.

EDRS PRICE MF01/PC04 Plus Postage.
 DESCRIPTORS *College Science: *Computer Programs: Engineering:
 *Engineering Education: Fuels: Higher Education:
 Hydraulics: *Learning Modules: Mathematical Models:
 Mechanics (Physics): *Nuclear Physics: Physics:
 *Science Education: Science Instruction:
 Thermodynamics

ABSTRACT

This learning module is concerned with the temperature field, the heat transfer rates, and the coolant pressure drop in typical liquid metal fast breeder reactor (LMFBR) fuel assemblies. As in all of the modules of this series, emphasis is placed on developing the theory and demonstrating the use with a simplified model. The heart of the module is the LMFBR Thermal-Hydraulics Computer Code which solves for the radial temperature distributions in the fuel, cladding, and coolant at any axial station and then marches axially with an energy balance in the coolant. The code and its use are described in detail, including a listing and definition of all variables, a discussion of all input requirements and resulting output, an annotated flow chart of the code, an explanation of all options in the code, and a listing of the code which includes enough comment statements to clearly indicate the operational steps being performed. By proper specification of the options, the code can either be used as an individual entity to study thermal-hydraulic aspects exclusively, or as a subroutine in the total LMFBR module package to provide temperature feedback to the other modules. Examples are worked out using the code. (Author/SK)

 * Reproductions supplied by EDRS are the best that can be made *
 * from the original document. *

THERMAL-HYDRAULICS MODULE, TH-2
LIQUID METAL FAST BREEDER REACTOR THERMAL-HYDRAULICS

by

Thomas C. Reihman

The University gratefully acknowledges the support of the
Division of Higher Education of the National Science Foundation
for support of this work performed under Grant GZ-2888 and the
support of Duke Power Company, North Carolina Power and Light Company,
and Virginia Electric and Power Company.

Project Director: Milton C. Edlund

3

DEC 12 1980

4-16

TABLE OF CONTENTS

	<u>Page</u>
1.0 Object of Module	1
2.0 Content of the Module.	2
3.0 LMFBR Fuel Geometry and Its Model.	4
4.0 LMFBR Thermal-Hydraulic Theory	9
4.1 Internal Heat Generation	9
4.2 Temperature Distribution in the Fuel	12
4.3 Temperature Distribution in the Cladding	17
4.4 Temperature Drop in the Convective Layer	19
4.5 Pressure Drop in the Coolant	22
4.6 The Heat Transfer Coefficient.	30
4.7 Incremental Energy Balances.	36
4.8 Assessment of Local Coolant Conditions	38
5.0 The LMFBR Thermal-Hydraulics Code.	39
5.1 Nomenclature	45
5.2 Code Input	50
5.3 Code Output.	53
5.4 Code Flow Chart.	54
5.5 Code Examples.	60
6.0 References	84
7.0 Problems	86

THERMAL-HYDRAULICS MODULE, TH-2

LIQUID METAL FAST BREEDER REACTOR THERMAL-HYDRAULICS

1.0 Object of Module

The object of this module is to present the basic elements of liquid metal fast breeder reactor thermal-hydraulics. This requires a demonstration of:

- How the actual fuel geometry can be modeled for simplified thermal-hydraulic analysis.
- What information is necessary to characterize the thermal-hydraulic behavior of the reactor.
- The development of the theoretical relations that permit the computation of these thermal-hydraulic characteristics.
- The actual calculation of this information for the reactor. This calculation requires the use of the LMFBR Thermal-Hydraulics Code, the description of which is included in this module.

The thermal-hydraulic characteristics of the reactor are required for the determination of:

- Fuel integrity
- Cladding integrity
- Coolant exit conditions
- Pumping requirements
- Temperature feedback for reactor neutronics calculations.

2.0 Content of the Module

This learning module contains the thermal-hydraulics of liquid metal fast breeder reactors. Specifically, the module is concerned with the temperature field, the heat transfer rates and the coolant pressure drop in typical LMFBR fuel assemblies.

As in all of the modules of this series, emphasis is placed on developing the theory and demonstrating its use with a simplified model. The model is carefully selected to insure that analyses based on it will exhibit all of the important thermal-hydraulic trends of the typical reactor. The description of the fuel for a typical LMFBR and the modeling of the fuel which preserves the significant thermal-hydraulic characteristics are treated in the next section of this module.

Following the geometry and modeling section, the basic theory governing the temperature distributions, heat transfer rates, pressure drops, and energy balance considerations is presented. The temperature distributions in the fuel and cladding are calculated assuming one-dimensional radial heat conduction. The pressure drop in the coolant channels and the heat transfer coefficient for use in Newton's law of cooling are calculated from empirical relations developed for reactor coolant channel flows. Energy balances for small axial segments of the coolant channel are used to step the solution in the axial direction. Simple examples, illustrating the individual calculations, are worked out in detail for typical LMFBR conditions.

The heart of the module is the LMFBR Thermal-Hydraulics Computer Code. Basically, the code solves for the radial temperature distributions in the fuel, cladding, and coolant at any axial station and then marches axially with an energy balance in the coolant. The code and its use are described in detail. Included are a listing and definition of all variables, a

discussion of all input requirements and resulting output, an annotated flow chart of the code, an explanation of all options in the code, and a listing of the code which includes enough comment statements to clearly indicate the operational steps being performed. By proper specification of the options, the code can either be used as an individual entity to study thermal-hydraulic aspects exclusively, or as a subroutine in the total LMFBR module package to provide temperature feedback to the other modules. Examples are worked out using the code. In typical examples, the location and magnitude of the maximum fuel temperature in the LMFBR are found and the effect of oversized cladding on maximum fuel temperature and coolant outlet temperature are determined.

3.0 LMFBR Fuel Geometry and Its Model

The typical LMFBR core is approximately cylindrical in shape and is composed of about 200 to 250 fuel assemblies. These fuel assemblies are hexagonal in cross section, 10 to 15 feet long, and stand vertically in the core. Small gaps separate the fuel assemblies from one another. The fuel assemblies are contained inside a core shroud which in turn fits inside a cylindrical core support which is 10 to 15 feet in diameter. To provide a flattening of the neutron flux (and hence the power production) in the radial direction, the enrichment of the fuel is varied in cylindrical zones. The individual fuel assemblies are orificed such that the coolant flow is proportional to the power generation of the assembly.

The fuel assembly consists of 150 to 275 fuel rods, support grids holding the rods firmly at the ends, and a hexagonal flow duct. The spacing between the individual rods and between the rods and the duct wall is maintained by helically wound wire wraps on the fuel rods. About 4 to 6 feet of the fuel rods contain nuclear fuel and therefore generate heat internally during reactor operation.

A cross-section of a typical fuel assembly is shown in Figure 1. The fuel rods are arranged in a triangular array within the fuel assembly. The liquid metal coolant, which carries away the energy generated within the fuel rods, flows in the spaces between the rods and between the rods and the duct. Three types of coolant channels can be identified as shown in Figure 1. These correspond to the channels associated with central fuel rods, outer row fuel rods, and corner fuel rods.

Note that a great majority (384 out of 438 coolant channels in a 217-pin bundle) of the coolant channels are central-type coolant channels. Also note that there are about two (actually 2.02) flow channels for each fuel rod.

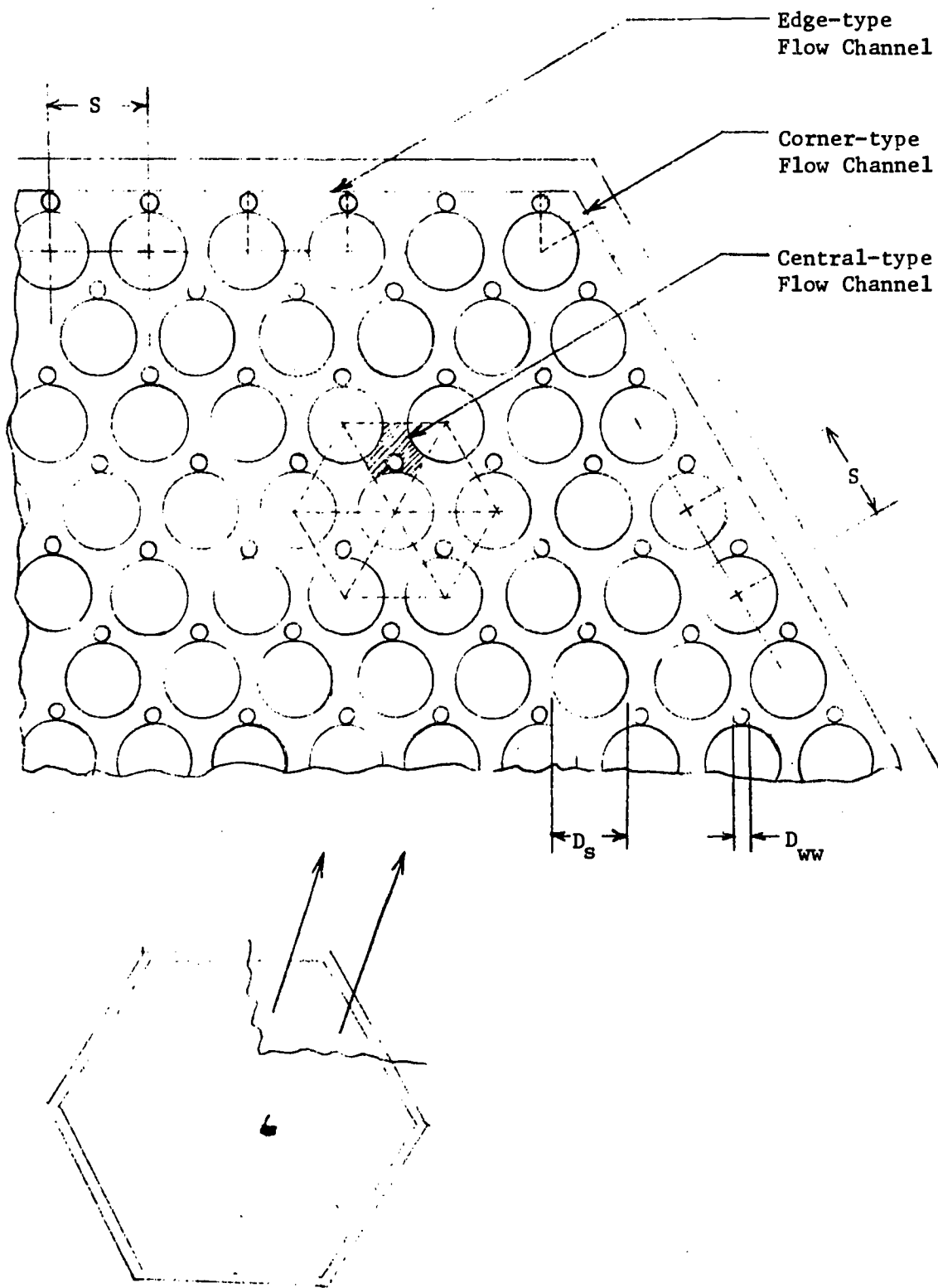


Figure 1. LMFBR Fuel Geometry.

Thus, to a reasonable approximation, the coolant passage associated with each fuel rod in the model can be taken as two central-type channels. The model flow passage per fuel rod, therefore, consists of two triangles, each with corners at the centers of the three fuel rods forming the channel minus the three sixty-degree segments of the fuel rods themselves. The ratio of center-to-center spacing, S , to the fuel rod diameter, D_s , is typically 1.1 to 1.3.

Each flow channel serves segments of three fuel rods as can be seen in Figure 1. Since the three rods are identical, and since the neutron flux does not vary significantly in the short distance from one rod to the next, all three rods may be assumed to have the same operating characteristics. Thus the three fuel rod segments associated with each flow channel can be treated as one-half equivalent fuel rod. The power generation level in this model fuel rod will be taken as that of the average fuel rod in the core.

The model fuel rod will have a variation in power density in the axial direction. This variation will be taken as

$$q'''(Z) = q'''_0 \cos \frac{\pi Z}{H_e} \quad (1)$$

unless a computed actual axial variation is provided from another module. In Equation 1, q''' represents the thermal source strength per unit volume at any axial location Z , q'''_0 represents the thermal source strength per unit volume at the center of the fuel rod ($Z=0$), and H_e is the extrapolated height of the core. Both q''' and q'''_0 are taken to be constant radially throughout the fuel in the fuel rod. The magnitude of q'''_0 is representative of that of the average fuel rod in the core. The extrapolated height is calculated from

$$H_e = H + 2 L_e \quad (2)$$

where H is the actual height of the reactor core and L_e is an extrapolation length. The extrapolation length is the distance between the actual end of the core and the location where an extrapolation of the waveform representing the actual neutron flux distribution within the core goes to zero. From neutron diffusion theory L_e can be shown to be about one migration length for a bare core. The migration length can be calculated from neutron diffusion theory [1,2,3].*

The LMFBR fuel rods are 10 to 15 feet long and about 0.25 to 0.30 inch in diameter. About 4 inches of the total length is used for end fittings, about 1 foot on each side of the active core consists of a blanket of depleted UO_2 , and about 3 to 5 feet near the downstream end serves as a fission gas plenum. The remaining length contains nuclear fuel, usually uranium dioxide and plutonium dioxide. The fuel is typically in the form of cylindrical pellets with a diameter of about 0.25 inch. These fuel pellets are stacked inside a tube of cladding, a stainless steel alloy with about a 0.02 inch thick wall. There is a 0.003 to 0.005 inch gap between the fuel and the inside of the cladding.

For simplicity, the gap is neglected in the model of the fuel rod. The model fuel rod thus consists of fuel of diameter D_f contained in a tube of cladding with an inside diameter D_f and an outside diameter D_s . For the model fuel rod, the length of the end fittings will each be assumed to be 3% of the active fuel length, the length of the blankets will each be assumed to be 20% of the active fuel length and the length of the gas plenum on the top of the fuel will be taken as 80% of the active fuel length.

*Numbers in brackets refer to items in References.

Each fuel rod is wound with a wire wrap to provide spacing and also to promote mixing between the coolant channels. For the typical S/D_s ratio of 1.2, the diameter of the wire wrap corresponds to 20% of the outside diameter of the cladding. The helical pitch with which the wire is wound on the rod is typically 1 foot.

The wire wrap on the fuel pins complicates the calculation of the equivalent diameter of the coolant channels. The wire wrap both reduces the flow area and adds to the wetted perimeter. In making the area and wetted perimeter calculations, it is important to note that there is a wire wrap inside a given flow channel for exactly 1/2 of the total axial distance. Thus it is reasonable to treat each flow channel as if 1/2 wire wrap were present at each axial level. The flow area and wetted perimeter then are

$$A_f = \frac{1}{2} S^2 \cos 30^\circ - \frac{\pi}{8} D_s^2 - \frac{\pi}{8} D_{ww}^2, \quad (3)$$

$$p_w = \frac{\pi}{2} (D_s + D_{ww}). \quad (4)$$

From these, the equivalent diameter of the coolant channel is given as

$$D_e = \frac{4A_f}{p_w}. \quad (5)$$

4.0 LMFBR Thermal-Hydraulic Theory

4.1 Internal Heat Generation

As a result of nuclear fission in the fuel, heat is generated. The rate of energy generation in the fuel per unit volume is called the "volumetric thermal source strength", q''' , and can be calculated from

$$q''' = E_f N_{ff} \bar{\sigma}_f \phi \quad (6)$$

where E_f is the energy released per fission reaction (energy dimensions), N_{ff} is the fissionable fuel density (fissionable nuclei per unit volume), $\bar{\sigma}_f$ is the effective fission microscopic cross section (dimensions of area), and ϕ is the neutron flux (neutrons per unit area per unit time). Note that q''' has dimensions of energy per unit volume. The details of this calculation of volumetric thermal source strength are found in Reactor Statics Module 8.

The volumetric thermal source strength varies throughout the reactor since ϕ , and perhaps N_{ff} , vary. For a cylindrical reactor, axial symmetry is generally a reasonable approximation. Therefore q''' reduces to a function of only the radius, R , and the axial position, Z . Across any single fuel rod, the change in q''' is small (due to small change in R) and q''' can therefore be considered constant across its cross section. Thus for any single fuel rod q''' is a function of only the axial position. Also for any small axial segment of a fuel rod (the order of 1% of the total active length) the change in q''' is moderate. Using a constant average value for any such segment thus introduce little error into the analysis. This approximation is used in this module.

The heat generation in any small segment of the fuel can be obtained by multiplying the volumetric thermal source strength by the volume of the

segment. For steady state conditions this energy must be removed from the fuel. The mechanism by which this heat transfer occurs within the fuel is thermal conduction.

Example 1.

A LMFBR containing 25,000 fuel rods generates 2000 Mw (t). The cylindrical core of the reactor is 5 ft long and 4 ft in diameter. The fuel consists of 0.22 in. diameter UO_2 fuel pellets. These are contained in cladding which has an outside diameter of 0.25 in. The fuel rods are spaced 0.30 in. center-to-center in a triangular array. The volumetric thermal source strength of the fuel varies as $q''' = q'''_0 \cos(\pi Z/H_e)$. The extrapolation length for the fuel is 3 in. Find the power per unit length (in kw/ft) and q'''_0 for the average fuel rod in the core.

Solution.

The power generated in the average fuel rod is

$$P_{ave} = \frac{P_{total}}{N} = \frac{2000 \times 10^6}{25,000} = 80,000 \text{ watt} = 80 \text{ kw.}$$

Thus, per unit length the power is $\frac{P}{L} = \frac{80 \text{ kw}}{5 \text{ ft}} = 16 \frac{\text{kw}}{\text{ft}}$.

The power produced by the average fuel rod can also be calculated by integrating the power produced in each differential volume of the fuel rod. Thus,

$$\begin{aligned} P_{ave} &= \int_V q''' dV = \int_{-H/2}^{H/2} q'''_0 \cos(\pi Z/H_e) (\pi D_f^2/4) dZ \\ &= (H_e D_f^2 q'''_0/4) [\sin(\pi Z/H_e)]_{-H/2}^{H/2} \\ &= (H_e D_f^2 q'''_0/2) \sin(\pi H/2H_e) \end{aligned}$$

Solving for q'''_o :

$$q'''_o = \frac{2P_{ave}}{H_e D_f^2 \sin(\pi H / 2H_e)}$$
$$= \frac{(2)(80,000 \text{ watt})(3.413 \frac{\text{Btu}}{\text{watt-hr}})}{(5.5 \text{ ft})(0.22 \text{ in.})^2 (\frac{1}{12} \frac{\text{ft}}{\text{in.}})^2 \sin[(\pi)(5 \text{ ft}) / (2)(5.5 \text{ ft})]}$$
$$= 2.98 \times 10^8 \text{ Btu/hr-ft}^3.$$

4.2 Temperature Distribution in the Fuel

For conduction heat transfer the heat flux is proportional to the normal temperature gradient. When the proportionality constant is inserted,

$$q_n = -kA_n \frac{\partial T}{\partial X_n} \quad (7)$$

where q_n is the heat transfer rate in the n-direction (energy/time), $\partial T/\partial X_n$ is the temperature gradient in the n-direction (degrees/length), A_n is the area normal to the n-direction, and k is the thermal conductivity of the material (energy/degree-length-time). Equation 7, which is Fourier's law of heat conduction, relates the heat transfer to the temperature field and is also the defining equation for the thermal conductivity. The thermal conductivity is a material property and its magnitude in general varies with the temperature of the material. Heat transfer properties of various reactor materials are tabulated as functions of temperatures in References 4 and 5. To reduce the complexity of heat transfer calculations, the thermal conductivity is often assumed to be constant and evaluated at an average temperature. The minus sign in Equation 7 assures that the heat transfer is in the direction of decreasing temperature. Equation 7 shows that temperature gradients are required for heat transfer. In nuclear reactor applications, where there are high heat transfer rates, large temperature variations occur. One of the primary tasks of reactor thermal-hydraulic analysis is the prediction of this temperature distribution in the fuel.

The heat conduction equation in cylindrical coordinates,

$$\frac{\partial^2 T}{\partial r^2} + \frac{1}{r} \frac{\partial T}{\partial r} + \frac{1}{r^2} \frac{\partial^2 T}{\partial \theta^2} + \frac{\partial^2 T}{\partial z^2} + \frac{q''' }{k} = \frac{1}{\alpha} \frac{\partial T}{\partial t}, \quad (8)$$

and the initial and boundary conditions prescribe the temperature distribution within the fuel rod. In this relation, the thermal conductivity, k , and the

thermal diffusivity, α , have been assumed constant. The development of this equation is found in heat transfer texts [4,5,6] and several simplified cases are given as exercises for the student. For steady state conditions, the unsteady term on the right hand side of the equation is zero, and for axial symmetry, the θ variation disappears. It may also be observed that since the length of a fuel pin is much greater than its radius, the temperature gradients in the radial direction will be much greater than the temperature gradients in the axial direction. Therefore, to a good approximation, the heat transfer in the axial direction can be neglected with respect to that in the radial direction, and the resulting temperature distribution and heat transfer reduced to a one-dimensional case for any axial segment in which q''' may be assumed constant. The governing differential equation for this case reduces to the ordinary differential equation

$$\frac{d^2T}{dr^2} + \frac{1}{r} \frac{dT}{dr} + \frac{q'''}{k_f} = 0 \quad (9)$$

The solution of Equation 9 subject to the boundary conditions

$$\begin{aligned} T &= T_o \text{ at } r = 0, \\ \frac{dT}{dr} &= 0 \text{ at } r = 0 \end{aligned} \quad (10)$$

yields the temperature distribution in the fuel. The second boundary condition is obtained from the observation that the temperature distribution must be continuous across the center of the cylinder. Observing that both q''' and k are constant and that

$$\frac{d^2T}{dr^2} + \frac{1}{r} \frac{dT}{dr} = \frac{1}{r} \frac{d}{dr} \left(r \frac{dT}{dr} \right) \quad (11)$$

Equation 9 can be written as

$$\frac{d}{dr} \left(r \frac{dT}{dr} \right) = - \frac{q'''}{k_f} r \quad (12)$$

Integrating twice results in

$$T = -\frac{q''''}{k_f} \frac{r^2}{4} + C_1 \ln r + C_2. \quad (13)$$

Applying the boundary conditions of Equation 10, the integration constants are

$$\begin{aligned} C_1 &= 0, \\ C_2 &= T_o. \end{aligned} \quad (14)$$

Substituting into Equation 13 gives

$$T = T_o - \frac{q''''}{4k_f} r^2. \quad (15)$$

This relation shows the temperature distribution in the fuel to be parabolic with maximum temperature at the center. The heat transfer rate through any cylindrical shell can be calculated from Fourier's law which takes the form

$$q_r = -k_f A_r \frac{dT}{dr} \quad (16)$$

where $A_r = 2\pi r(\Delta L)$, ΔL being the length of the cylindrical shell.

Of particular interest are the temperature and heat transfer at the surface of the fuel; i.e., at $r = r_f = D_f/2$. At this location,

$$T_f = T_o - \frac{q''''}{4k_f} r_f^2, \quad (17)$$

$$\begin{aligned} q_f &= -k_f 2\pi r_f (\Delta L) \left. \frac{dT}{dr} \right|_{r=r_f} \\ &= \pi r_f^2 (\Delta L) q'''' . \end{aligned} \quad (18)$$

Noting that $\pi r_f^2 \Delta L$ is the volume of the fuel rod segment of length ΔL it is observed that the heat transfer out of the $r = r_f$ cylindrical shell is indeed equal to the total energy generated as calculated from (q'''') (fuel volume). For one-dimensional heat transfer all of the energy generated within the fuel must be transferred out through the surface.

Example 2.

Equation 17 relates the temperatures at the center and surface of a heat-generating cylindrical fuel rod. This equation contains the thermal conductivity of the fuel which, in general, is a function of temperature. However, the analysis leading to Equation 17 assumes the thermal conductivity to be constant. Determine the temperature at which to evaluate k_f to make the assumption of constant k_f compatible with a k_f that varies linearly with temperature.

Solution.

The method of solution is to develop an expression relating T_o and T_s which assumes $k_f = a + bT$ and then compare this result with Equation 17. We begin with Fourier's law of heat conduction,

$$q = -k_f A \frac{dT}{dr}.$$

Recognizing that $q = q'''(\text{volume})$ and $A_r = 2\pi r(\Delta L)$:

$$q''' \pi r^2 (\Delta L) = k_f 2\pi r (\Delta L) \frac{dT}{dr}.$$

Simplifying, separating variables, and substituting for k_f :

$$q''' r dr = -2(a + bT) dT.$$

Integrating from $r = 0$ to $r = r_f$ with q''' , a , b constant,

$$q''' \left[\frac{r^2}{2} \right]_0^{r_f} = -2 \left[aT + \frac{b}{2} T^2 \right]_{T_o}^{T_f}$$

$$q''' \frac{r_f^2}{4} = -a(T_f - T_o) - \frac{b}{2}(T_f^2 - T_o^2)$$

$$= \left[a + \frac{b}{2}(T_o + T_f) \right] (T_o - T_f)$$

$$T_o - T_f = \frac{q''' r_f^2}{4[a + \frac{b}{2}(T_o + T_f)]}$$

Comparing this with Equation 17 written as

$$T_o - T_f = \frac{q''' r_f^2}{4 k_f}$$

we see that the relations are equivalent for

$$k_f = a + \frac{b}{2}(T_o + T_f).$$

Note that this is precisely equal to k_f evaluated at the arithmetic average fuel temperature; i.e., $k(\frac{T_o + T_f}{2})$.

4.3 Temperature Distribution in the Cladding

The temperature distribution in the cladding can be calculated by methods similar to those used for the fuel. Noting that no energy is generated in the fuel, the governing equation simplifies to

$$\frac{d}{dr} \left(r \frac{dT}{dr} \right) = 0. \quad (19)$$

The boundary conditions obtained by matching temperature and heat transfer at the fuel-cladding interface are

$$\begin{aligned} T &= T_f \text{ at } r = r_f, \\ \frac{dT}{dr} &= - \frac{q_f}{2\pi k_c r_f (\Delta L)} = - \frac{r_f q'''}{2k_c} \text{ at } r = r_f \end{aligned} \quad (20)$$

where k_c is the thermal conductivity of the cladding.

Integrating Equation 19 twice yields

$$T = C_3 \ln r + C_4. \quad (21)$$

Applying the boundary conditions in Equation 20,

$$\begin{aligned} C_3 &= - \frac{r_f^2 q'''}{2k_c}, \\ C_4 &= T_f + \frac{r_f^2 q'''}{2k_c} \ln r_f. \end{aligned} \quad (22)$$

Substituting into Equation 21 yields the temperature distribution in the cladding,

$$T = T_f - \frac{r_f^2 q'''}{2k_c} \ln \frac{r}{r_f}. \quad (23)$$

Or, if q''' is eliminated in favor of q_f ,

$$T = T_f - \frac{q_f}{2\pi k_c (\Delta L)} \ln \frac{r}{r_f}. \quad (24)$$

The temperature at the surface of the cladding, T_s , is obtained by evaluating Equation 24 at r_s ,

$$T_s = T_f - \frac{q_f}{2\pi k_c (\Delta L)} \ln \frac{r_s}{r_f} . \quad (25)$$

Note also that the same heat transfer rate must occur through each cylindrical layer for the steady state conditions; i.e., $q_f = q_s$.

4.4 Temperature Drop in the Convective Layer

All of the heat generated within the fuel ultimately must be transferred to the coolant. Thus, all of this energy must be transferred through the fluid layer near the outer surface of the cladding. The heat transfer mechanism, wherein the energy is carried away or convected from the solid surface by a fluid in motion, is called convection. The heat transfer rate for convective heat transfer is related to the temperature difference between the surface and the bulk fluid, the driving potential for the heat transfer, by Newton's law of cooling,

$$q_s = h A_s (T_s - T_B). \quad (26)$$

This relation may also be taken as the defining equation for the heat transfer coefficient, h . The bulk temperature, T_B , is a mass-weighted average temperature of the fluid in the flow channel. It is formally defined by

$$T_B = \frac{\int_A \rho C_p U T \, dA}{\dot{m} C_p}. \quad (27)$$

This is the temperature that a thermometer would indicate if immersed in the mixed fluid collected from the discharge of the flow channel at the given location.

Relations for calculating h from the flow characteristics and coolant properties have been developed. These will be treated in a later section of the module. For the moment, the quantity of interest is the temperature drop across the convective layer. In terms of h this can be obtained from Equation 26 as

$$T_s - T_B = \frac{q_s}{2\pi r_s (\Delta L) h} \quad (28)$$

where r_s is the outer radius of the cladding.

Example 3.

Consider the LMFBR described in Example 1. The bulk temperature of the coolant changes from 665 F to 1335 F as the coolant flows through the reactor. Given that the heat transfer coefficient is 44,000 Btu/hr-ft²-F, the thermal conductivity of the cladding is 12.45 Btu/hr-ft-F, and the thermal conductivity of the fuel is 2.00 Btu/hr-ft-F, determine the fuel centerline temperature at the axial center of the core.

Solution.

Half of the total energy transfer to the coolant occurs in the first half of the core. Thus the coolant bulk temperature at the axial center of the core is 1000 F. To this, we must add the temperature rises across the convective layer, the cladding, and the fuel to obtain the fuel centerline temperature.

The heat transfer rate through the convective layer at $Z = 0$ is

$$\begin{aligned} q_s &= q''_o \text{ (fuel volume)} = q''_o \pi D_f^2 (\Delta L) / 4 \\ &= 2.98 \times 10^8 \text{ Btu/hr-ft}^3 (\pi/4) (0.22 \text{ in.})^2 (\text{ft}/12 \text{ in.})^2 (\Delta L \text{ ft}) \\ &= 78,784 (\Delta L) \text{ Btu/hr.} \end{aligned}$$

From Equation 26,

$$\begin{aligned} T_s - T_B &= \frac{q_s}{h A_s} = \frac{78784 \Delta L \text{ Btu/hr}}{(44,000 \text{ Btu/hr-ft}^2\text{-F}) \pi (0.25 \text{ in.}) (\text{ft}/12 \text{ in.}) (\Delta L \text{ ft})} \\ &= 27.3 \text{ F.} \end{aligned}$$

The heat transfer rate through the cladding is the same as that through the convective layer. Equation 25 yields

$$\begin{aligned} T_f - T_s &= \frac{q_f}{2\pi k_c (\Delta L)} \ln \frac{r_s}{r_f} \\ &= \frac{(78784 \Delta L \text{ Btu/hr}) \ln(0.125/0.11)}{2\pi(12.45 \text{ Btu/hr-ft-F})(\Delta L \text{ ft})} \\ &= 128.7 \text{ F.} \end{aligned}$$

From Equation 17 the temperature rise through the fuel is found as

$$\begin{aligned} T_o - T_f &= \frac{q''' r_f^2}{4 k_f} = \frac{2.98 \times 10^8 (\text{Btu/hr-ft}^3) (0.11 \text{ in.})^2 (\text{ft}/12 \text{ in.})^2}{4(2.00 \text{ Btu/hr-ft-F})} \\ &= 3130.0 \text{ F.} \end{aligned}$$

Adding these temperature rises to the bulk temperature,

$$\begin{aligned} T_o &= (T_o - T_f) + (T_f - T_s) + (T_s - T_B) + T_B \\ &= 3130.0 + 128.7 + 27.3 + 1000 = 4280.0 \text{ F.} \end{aligned}$$

4.5 Pressure Drop in the Coolant

All of the energy generated by nuclear fission in the fuel must be carried out of the reactor by the coolant which flows in the channels between the fuel rods. In LMFBR the coolant is a liquid metal which is force-circulated by a pump. Enough pressure head must be provided by the pump to overcome the pressure losses in the flow loop. The entire loop consists of the reactor flow channels, the heat exchangers, coolant purity maintenance components and connecting piping. Of interest here is the determination of the pressure loss incurred in the flow through the reactor core. Two types of pressure losses will be considered. These are the frictional pressure loss along the coolant channel and the entrance and exit permanent pressure losses.

The frictional pressure loss is a manifestation of the shear stress on the flowing fluid by the walls of the flow channel. This pressure loss is calculated from

$$\Delta P_F = f \frac{\Delta L}{D_e} \frac{\rho U_B^2}{2g_c} . \quad (29)$$

This relation may also be interpreted as the defining equation for the friction factor, f . The bulk velocity, U_B , found in Equation 29 is the velocity averaged across the flow channel. It is defined by

$$U_B = \frac{1}{A} \int_A U \, dA. \quad (30)$$

This velocity is related to the mass flow rate by

$$\dot{m} = \rho A U_B \quad (31)$$

or to the mass velocity by

$$G = \frac{\dot{m}}{A} = \rho U_B. \quad (32)$$

The equivalent diameter, D_e , is used to relate experimental data from circular tubes, which is abundant in the literature, to different geometries. The equivalent diameter is calculated from

$$D_e = \frac{4A_f}{p_w} . \quad (5)$$

Note that for a circular cross section the flow area is $\pi D^2/4$ and $p_w = \pi D$. Thus for a circle the equivalent diameter is equal to the actual diameter, as required. This, of course, is why the definition of Equation 5 is used.

The value of the friction factor depends on the flow and surface conditions in the channel. The flow conditions are characterized by the Reynolds Number,

$$Re = \frac{\rho U_B D_e}{\mu} . \quad (33)$$

It is well known that for Re below a critical value the flow is laminar, and for Re above the critical value the flow is turbulent. For internal flows this critical Re is about 2000. Laminar flow may be thought of as an ordered process in which fluid layers slide over one another, being retarded only by the molecular interaction between the layers. The viscosity of the fluid quantifies the magnitude of this interaction. In laminar flow any disturbance in the fluid is damped by the viscous action. In turbulent flow there is an additional random transport mechanism operable. This mechanism may be modeled as eddies (finite sized patches of fluid which retain their characteristics for finite times) moving throughout the fluid, transporting mass, momentum, and energy by virtue of their movement. This action is quite violent and results in transport rates much greater than those by purely molecular activity in laminar flow. In turbulent flow, disturbances in the flow field grow and propagate resulting in increased

turbulence levels downstream of the disturbances. Even in highly turbulent flows, there exists a layer near the solid bounding surfaces where the presence of the wall retards the penetration of eddies and therefore acts as a flow stabilizer. This results in a laminar sublayer existing near any solid boundary. Even though this layer is very thin, it is very important, since much of the temperature and velocity change between wall and bulk conditions occurs in this layer. In reactor coolant channels the flow is highly turbulent and Re of the order of 100,000 are quite common.

The surface conditions of the flow channel is characterized by the ratio of the surface roughness height to the equivalent diameter of the flow channel, ϵ/D_e . The flow channel exhibits smooth tube behavior if the roughness height is less than the thickness of the laminar sublayer. For reactor coolant flow channels the surface conditions are controlled so that this criterion is met.

The calculation of the friction factor for the reactor coolant flow channels is a three-step procedure. First the smooth circular tube friction factor is determined, then a correction factor is applied to account for the actual channel shape, and then a correction factor is applied to account for the wire-wrap spacers. The smooth circular tube friction factor can be determined from a Moody chart where f_{circ} is plotted versus Re . These charts are found in most fluid mechanics texts and handbooks [7,8,9,10]. An alternate method is to calculate the friction factor from a correlation in equation form. One of the most widely accepted for reactor work is

$$f_{circ} = \frac{0.184}{Re^{0.2}} \quad (34)$$

This relation, like the Moody diagram, was obtained from a curve fit of experimental data in smooth circular tubes. The friction factor defined in

this module is the Darcy-Weisbach friction factor. Care must be taken not to confuse this friction factor with the Fanning friction factor ($f_{\text{Fan}} = f_{\text{D-W}}/4$) also found in the literature.

A correction of the circular tube data to the rod bundle geometry has been obtained by Deissler and Taylor [11]. Their results, expressing f_o/f_{circ} as a function of S/D_s , can be approximated by the following polynomial fit:

$$f_o/f_{\text{circ}} = -3.475 + 8.053 \frac{S}{D_s} - 4.705 \left(\frac{S}{D_s}\right)^2 + 0.9162 \left(\frac{S}{D_s}\right)^3 \quad (35)$$

The correction for the wire-wrap spacer on the friction factor is quite significant. This correction may increase the smooth channel value by the order of 30% for typical LMFBR applications. The most extensive pressure drop data on wire-wrapped reactor fuel bundles in LMFBR operating ranges is that of Reihman [12]. His data show the effects of wire-wrap size, channel equivalent diameter, and wire-wrap helical pitch. The results may be approximated in polynomial form by

$$f/f_o = 1.195 - (HP - 0.75) \left[0.554 - 5.456 \frac{D_{\text{ww}}}{D_e} + 11.58 \left(\frac{D_{\text{ww}}}{D_e}\right)^2 \right] \quad (36)$$

The permanent pressure losses at the inlet and exit of the individual flow channels are the result of increased viscous energy dissipation resulting from increased turbulent activity. These losses may be calculated from

$$\Delta P_E = K \frac{\rho U_B^2}{2g_c} \quad (37)$$

In this relation K is the resistance coefficient for the inlet or exit geometry. The inlet may be approximated as a sudden contraction from a very large diameter to the equivalent diameter of the flow channel. For this sudden contraction, the resistance coefficient is 0.5 [10]. Similarly the

exit may be approximated as a sudden expansion from D_e to a very large diameter. For this expansion, K is 1.0 [10].

For each fuel assembly there is an additional pressure loss due to orificing. This additive pressure loss is omitted in this module, not because it is unimportant, but because its calculation requires specific design information on the individual fuel assemblies.

Example 4.

The LMFBR described in Example 1 has an inlet coolant temperature of 665 F, an inlet coolant pressure of 200 psia, and a coolant mass velocity of 7.0×10^6 lbm/hr-ft². The coolant exit temperature is 1335 F. Estimate the frictional pressure loss in the core.

Solution.

The coolant properties are evaluated at the average coolant temperature. At 1000 F:

$$\mu = 0.505 \text{ lbm/hr-ft},$$

$$\rho = 51.19 \text{ lbm/ft}^3.$$

The average coolant velocity is found from

$$U_B = G/\rho = (7.0 \times 10^6 \text{ lbm/hr-ft}^2)/(51.19 \text{ lbm/ft}^3) = 136,800 \text{ ft/hr}.$$

The equivalent diameter is computed next.

$$\begin{aligned} A_f &= \frac{1}{2} S^2 \cos 30^\circ - \frac{\pi}{8}(D_s^2 + D_{ww}^2) \\ &= 1/2(0.300 \text{ in.})^2(0.866) - \frac{\pi}{8}[(0.250 \text{ in.})^2 + (0.050 \text{ in.})^2] \\ &= 0.0134 \text{ in.}^2 \end{aligned}$$

$$P_w = \frac{\pi}{2}(D_s + D_{ww})$$
$$= \frac{\pi}{2}[(0.250 \text{ in.}) + (0.050 \text{ in.})] = 0.471 \text{ in.}$$

$$D_e = 4 A_f / P_w = 4(0.0134 \text{ in.}^2) / (0.471 \text{ in.})$$
$$= 0.114 \text{ in.} = 0.00948 \text{ ft.}$$

The Reynolds number is

$$Re = U_B D_e \rho / \mu$$
$$= (136,800 \text{ ft/hr})(0.00948 \text{ ft})(51.19 \text{ lbm/ft}^3) / (0.505 \text{ lbm/hr-ft})$$
$$= 131,400.$$

Using a circular tube friction factor correlation,

$$f_{\text{circ}} = 0.184 / Re^{0.2} = 0.184 / (131,400)^{0.2}$$
$$= 0.0174.$$

Applying the correction for the actual reactor flow channel,

$$f_o = f_{\text{circ}} [- 3.475 + 8.053(S/D_s) - 4.705(S/D_s)^2 + 0.916(S/D_s)^3]$$
$$= (0.0174) [- 3.475 + 8.053(\frac{0.45}{0.35}) - 4.705(\frac{0.45}{0.35})^2 + 0.916(\frac{0.45}{0.35})^3]$$
$$= 0.0183.$$

Applying the correction for the wire wrap,

$$f = f_o [1.195 - (0.186 - 1.364(D_{ww}/D_s) + 2.894(D_{ww}/D_e)^2)(HP - 0.75 \text{ ft}) / 0.25 \text{ ft}]$$

$$= (0.0183) [1.195 - (0.186 - 1.364 \left(\frac{0.050 \text{ in.}}{0.114 \text{ in.}} \right) + 2.894 \left(\frac{0.050 \text{ in.}}{0.114 \text{ in.}} \right)^2) \\ (1 \text{ ft} - 0.75 \text{ ft}) / (0.25 \text{ ft})] \\ = 0.0192 .$$

From the defining equation for the friction factor,

$$\Delta P_F = f(\Delta L/D_e) \rho U_B^2 / 2g_c \\ = (0.0192)(60 \text{ in.} / 0.114 \text{ in.})(51.19 \text{ lbm/ft}^3)(136,800 \text{ ft/hr})^2 \\ / (3600 \text{ sec/hr})^2 (2)(32.2 \text{ lbm-ft/sec}^2\text{-lbf}) \\ = 11600 \text{ lbf/ft}^2 \\ = 80.5 \text{ psi} .$$

Example 5.

Each coolant channel in a fuel assembly has the same pressure drop. If all coolant channels are not identical the flow will redistribute such that this equal pressure drop is attained. Determine the relation between average velocity in the coolant channel (or equivalently the mass velocity) and the equivalent diameter of the channel which governs the flow distribution. Neglect the effect of the equivalent diameter in the wire wrap friction multiplier.

Solution.

The frictional pressure drop is given by

$$\Delta P = f \frac{\Delta L}{D_e} \frac{\rho U_B^2}{2g_c} .$$

Substituting for the friction factor,

$$\Delta P = \frac{0.184}{Re^{0.2}} \frac{\Delta L}{D_e} \frac{\rho U_B^2}{2g_c}$$
$$= \frac{0.184}{\left[\frac{U_B D_e \rho}{\mu} \right]^{0.2}} \frac{\Delta L}{D_e} \frac{\rho U_B^2}{2g_c}$$

$$\propto U_B^{1.8} / D_e^{1.2}$$

if constant density and viscosity are assumed. For channels 1 and 2, each having equal pressure drop,

$$U_{B1}^{1.8} / D_{e1}^{1.2} = U_{B2}^{1.8} / D_{e2}^{1.2}$$

or

$$U_{B2} / U_{B1} = (D_{e2} / D_{e1})^{2/3}$$

4.6 The Heat Transfer Coefficient

The usual relations for heat transfer coefficient developed for water, air, and similar "normal" substances can not be used for liquid metals. The reason is that the Prandtl number range of liquid metals (typically 0.001 to 0.01) is vastly different than that of the other substances (typically 0.7 to 30). Consequently, analyses based on the assumption that $Pr = 1$ and correlations obtained from data in the 0.7 to 30 range of Pr could not be expected to yield even order of magnitude results.

The Prandtl number is defined as the ratio of the molecular diffusivity of momentum to the molecular diffusivity of heat; i.e., $Pr = \nu/\alpha$ where $\nu = \mu/\rho$ and $\alpha = k/\rho C_p$. The Pr of liquid metals is very low compared to that of other fluids because of the very high thermal conductivities (typically 40 Btu/hr-ft-F compared to 0.1 Btu/hr-ft-F). The Prandtl number relates the temperature field to the velocity field. The low value of Pr for liquid metals indicates that the velocity field is relatively unimportant in the establishment of the temperature field in the fluid. The low value of Pr also indicates that the resistance to heat transfer is now distributed more uniformly through the fluid rather than largely concentrated in the laminar-sublayer as it is for higher Pr fluids. Thus, it should be apparent that liquid metal heat transfer is significantly different than that in ordinary fluids.

For turbulent flow in circular tubes with uniform heat input several correlations appear in the literature [13,14,15,16]. Of these, perhaps the best known is the Lyon-Martinelli relation [13,16],

$$Nu = 7 + 0.025 Pe^{0.8} . \quad (38)$$

The two dimensionless moduli in the equation are the Nusselt number,

$$\text{Nu} = \frac{hD}{k}, \quad (39)$$

and the Peclet number,

$$\text{Pe} = \text{Re Pr} = \frac{U_B D \rho C_p}{k} = \frac{U_B D}{\alpha}, \quad (40)$$

One common interpretation of the Nu is that it is the ratio of the actual heat transfer from a surface to the heat transfer that would result by molecular conduction through the stagnant fluid. The Pe, rather than the Re and Pr individually, is common to all liquid metal heat transfer coefficient correlation equations. This grouping eliminates the viscosity from the correlation and thereby signifies that the viscosity is not rate-determining in liquid metal heat transfer. The theoretical basis of the Lyon-Martinelli relation stems from the analogy of heat and momentum transfer by Martinelli [16]. Lyon [13] assumed that the turbulent eddy conductivity of heat is negligible compared to the high molecular conductivity of liquid metals and obtained the simplified result of Equation 38.

Another common liquid metal heat transfer correlation for circular tubes is that of Lubarsky and Kaufman [14],

$$\text{Nu} = 0.625 \text{Pe}^{0.4}. \quad (41)$$

This relation was obtained by carefully analyzing and reevaluating all the existing liquid metal heat transfer data at the time and then obtaining the best fit to the data. This relation predicts considerably lower values of Nu than Equation 38. Since this is the more conservative result, the use of Equation 41 rather than Equation 38 is recommended. It should be pointed out however, that the prediction of heat transfer coefficient for

liquid metal systems is not a precise science. Even after rejecting some data for oxide contamination, the remaining data shows deviations of up to $\pm 50\%$ from the values predicted by the correlations.

Heat transfer coefficient data for flow parallel to rod bundles is limited. The only experimental data in the LMFBR range of S/D_s is that of Borishansky and Firsova [17] and Subbotin et al. [18] and there are serious questions as to oxide contamination and surface wetting problems in these data. Also, since the velocity field and temperature field are not strongly coupled for low Pr fluids, the multiplicative friction factor correction of Deissler and Taylor [11] does not apply. Therefore reliance will be placed on the analytical work of Dwyer [19] in which he predicts Nu for liquid metals in fully developed turbulent flow in staggered rod bundles with uniform heat flux. Fortunately, Dwyer's results are directly applicable to the low S/D_s range (1.1 to 1.3) of the LMFBR. There is some experimental verification of Dwyer's predictions in that they agree well with the data of Borishansky and Firsova for $S/D_s = 1.2$ and Pe greater than 200. The final results of Dwyer's work are somewhat limited due to the lengthy computational time required. The results that are available can be approximated in the following form which is convenient for use in the LMFBR Thermal Hydraulics Code:

$$Nu = \begin{cases} Nu_o & \text{for } Pe \leq Pe_o \\ Nu_o + 0.025(Pe - Pe_o)^{0.8} & \text{for } Pe > Pe_o \end{cases} \quad (42)$$

where

$$Nu_o = - 88.0 + 130.8 \frac{S}{D_s} - 41.67 \left(\frac{S}{D_s}\right)^2, \quad (43)$$

$$Pe_o = 336 \frac{S}{D_s} - 110. \quad (44)$$

This approximation, in which the equivalent diameter is to be used in the Nu and Pe, is expected to fit the results of Dwyer within 15% in the range of S/D_s from 1.1 to 1.5 and the Pe range from 30 to 3000.

The above results apply strictly only to staggered rod bundles without wire wraps. There is no data in the literature on the heat transfer characteristics of wire-wrapped bundles. One could postulate various effects of the wire wraps on the heat transfer coefficient. For instance, the increased turbulence from the wire wraps would tend to increase the heat transfer. But for liquid metals where molecular conduction far outweighs eddy conduction one would expect this effect to be secondary. The wire wraps also add appreciable heat transfer area (S/D_s times the unwrapped area). However, any heat transfer into the liquid metal through the wire wrap would experience resistance to heat transfer in the wire wrap itself and a contact resistance between the wire wrap and the cladding. Finally, there is an effect via the equivalent diameter, the wire-wrapped bundle having a substantially smaller equivalent diameter. Thus, when the heat transfer coefficient is calculated from the Nusselt number, a larger value of h will result. There is also a secondary effect in the opposite direction in that Pe will be smaller. The effect just described via the equivalent diameter can be justified physically. The smaller flow channel has a lower thermal resistance between the wall and an "average" fluid particle in the channel (since the mean distance is smaller). The procedure recommended and the one used in the LMFBR Thermal-Hydraulics Code is to use the equivalent diameter calculated with the wire wrap in place and neglect the other two possible "corrections" on the heat transfer.

Example 6.

Determine the average heat transfer coefficient for the LMFBR described in Examples 1 and 4.

Solution.

The average heat transfer coefficient corresponds closely to that calculated at the average coolant conditions; i.e., 1000 F and 160 psia. Additional fluid properties required for this calculation are

$$C_p = 0.312 \text{ Btu/lbm-F,}$$

$$k = 37.62 \text{ Btu/hr-ft-F.}$$

The Prandtl number is

$$Pr = C_p \mu / k$$

$$= (0.312 \text{ Btu/lbm-F})(0.505 \text{ lbm/hr-ft}) / 37.62 \text{ Btu/hr-ft-F}$$

$$= 0.00419 .$$

Computing the Peclet number ,

$$Pe = Re Pr = (131,400)(0.00419) = 550.3 .$$

Applying the Nu correlation for reactor flow channels ,

$$Pe_o = 336.0(S/D_s) - 110.0$$

$$= 336.0(0.300 \text{ in.}/0.250 \text{ in.}) - 110.0$$

$$= 293.2$$

$$Nu_o = - 88.0 + 130.8(S/D_s) - 41.67(S/D_s)^2$$

$$\begin{aligned} &= - 88.0 + 130.8(0.300 \text{ in.}/0.250 \text{ in.}) - 41.67(0.300 \text{ in.}/0.250 \text{ in.})^2 \\ &= 8.955 \end{aligned}$$

$$\begin{aligned} \text{Nu} &= \text{Nu}_o + 0.025(\text{Pe} - \text{Pe}_o)^{0.8} \\ &= 8.955 + 0.025(550.3 - 293.2)^{0.8} \\ &= 11.073 . \end{aligned}$$

Calculation of h from the definition of Nu gives

$$\begin{aligned} h &= (\text{Nu}) k/D_e \\ &= (11.073) (37.62 \text{ Btu/hr-ft-F}) / (0.00948 \text{ ft}) \\ &= 43,940 \text{ Btu/hr-ft}^2\text{-F} . \end{aligned}$$

4.7 Incremental Energy Balances

As heat is transferred from the fuel rod to the coolant, the temperature of the coolant rises. Thus, the coolant temperature varies from a minimum at the inlet of the coolant channel to a maximum at the exit of the fuel bundle. The bulk temperature at any axial position can be determined from an energy balance where the total energy added by heat transfer to the coolant is equated to the energy rise of the coolant; i.e.,

$$\dot{m}i = \dot{m}i_{in} + \int_{-H/2}^Z q_s(z) dz. \quad (45)$$

Recognizing that for liquid metals $\Delta i = C_p \Delta T_B$ and solving for the local bulk temperature, this becomes

$$T_B = T_{in} + \frac{1}{\dot{m}C_p} \int_{-H/2}^Z q_s(z) dz \quad (46)$$

Equation 46 can be used to determine the bulk temperature increase for any segment, ΔL , of the coolant channel by

$$T_{B2} - T_{B1} = \frac{1}{\dot{m} C_p} \int_{Z_c - \Delta L/2}^{Z_c + \Delta L/2} q_s(z) dz \quad (47)$$

where Z_c is the center of the increment under consideration. Defining an average surface heat flux for the increment, $\bar{q}_s'' = \bar{q}_s / A_s$, the incremental bulk temperature rise becomes

$$T_{B2} - T_{B1} = \frac{\pi D_s \Delta L}{\dot{m} C_p} \bar{q}_s'' \quad (48)$$

The local surface heat flux, $q_s''(z)$, is related to the local volumetric thermal source strength by observing that all of the energy generated in the fuel is transferred out through the surface of the cladding; i.e.,

$$\pi D_s dZ q_s''(z) = \frac{\pi}{4} D_f^2 dZ q''''(z). \quad (49)$$

This simplifies to

$$q_s''(z) = \frac{D_f^2}{4D_s} q''''(z). \quad (50)$$

Similarly,

$$q_s'' = \frac{D_f^2}{4D_s} q'''' . \quad (51)$$

4.8 Assessment of Local Coolant Conditions

The current generation LMFBR's are designed to operate with no boiling of the liquid metal coolant. This requires that at every point in the flow the liquid metal temperature must be lower than its saturation temperature at the local pressure.

The maximum coolant temperature at any cross section of the reactor flow channel occurs in the fluid layer immediately adjacent to the cladding. The magnitude of this temperature approaches the outer surface temperature of the cladding. Thus, the criterion for the absence of boiling in the reactor is that the cladding surface temperature at all points be lower than the saturation temperature of the liquid metal at that level in the reactor.

The axial location of the maximum cladding surface temperature can be obtained by writing an expression for $T_s(Z)$ in terms of q''_o , H_e , D_f , D_s , \dot{m} , C_p , and h , differentiating with respect to Z , setting the derivative equal to zero, and solving for Z_m . The maximum cladding surface temperature can then be obtained by evaluating $T_s(Z)$ at Z_m . The details of this calculation are left as an exercise for the student. Unless the rate of decrease of the saturation temperature with axial position (due to frictional pressure drop) is appreciable, the critical point to check for surface boiling is near Z_m .

If the variation of cladding surface temperature and saturation temperature with axial position are known, it is a simple matter to visually check these data for the possibility of surface boiling. The output of the LMFBR Thermal-Hydraulics Code includes this information.

5.0 The LMFBR Thermal-Hydraulics Code

The LMFBR Thermal-Hydraulics Code calculates the thermal-hydraulic performance parameters discussed in Section 4 for the LMFBR model described in Section 4. The basic operational steps of the code are listed below.

1. Real \leftrightarrow integer conversions
2. Definition of statement functions
3. Accept and print input
4. Calculate flow area and equivalent diameter of coolant channel
5. Determine calculation increment
6. Calculate inlet pressure loss
7. Initialize to 1st calculation increment
8. Calculate bulk temperature rise and average temperature for 1st increment
9. Calculate average coolant properties for 1st increment
10. Calculate pressure loss for 1st increment
11. Calculate average pressure and saturation temperature for 1st increment
12. Calculate heat transfer coefficient for 1st increment
13. Calculate cladding outer surface temperature for 1st increment
14. Check for surface boiling for 1st increment
15. Calculate temperature distribution in fuel for 1st increment
16. Print 1st increment output
17. Repeat steps 7-16 for remaining increments
18. Calculate exit pressure loss and total pressure loss
19. Print coolant exit conditions.

The details of these specific steps requiring further explanation are found in the discussion below. A flow chart showing the calculations and logic is given in Section 5.4.

Most of the statement functions are used for convenience in calculating property data. These statement functions are in the form of some property, either of the coolant, cladding, or fuel, as a function of the corresponding temperature. All of the function forms are polynomials obtained by fitting polynomials of various degree to tabulated data. The order of these polynomials varies, having been selected to insure that the fit is accurate to within 2% over the range of interest of the parameter.

A detailed discussion of the input requirements is deferred until Section 5.2. For the moment it suffices to note that this input is supplied on three cards; one each for the geometry, the inlet flow conditions, and the reactor power level.

Since the cross section of the model flow channel does not change with axial position, the flow area and equivalent diameter are constant axially. The flow area is calculated from

$$A_f = \frac{1}{2} S^2 \cos 30^\circ - \frac{\pi}{8} D_s^2 - \frac{\pi}{8} D_{ww}^2. \quad (3)$$

The wire wrap diameter is related to S and D_s by

$$D_{ww} = S - D_s. \quad (52)$$

The equivalent diameter is then calculated from

$$D_e = \frac{4A_f}{P_w} \quad (5)$$

where the wetted perimeter is given by

$$P_w = \frac{\pi}{2} (D_s + D_{ww}). \quad (4)$$

In the code, the model coolant channel and fuel rod are sliced into short segments which are stacked axially to form the proper length core. The actual length of these segments is selected as a compromise between the very short segments for which the assumption of constant properties over the section axially is accurate and the very long segment which minimizes the computer time. An increment size equal to 1/100 of the active core length is built into the code. To study the effect of increment size, or to save computer time, this can readily be changed by altering two lines of the code.

After the increment size has been computed, the coolant conditions at the beginning of the first increment are established. The bulk temperature and mass velocity at the entrance of the first increment are set equal to the core inlet conditions provided in the input. The pressure at the entrance of the first calculation increment is obtained by subtracting the inlet pressure loss, computed from Equation 29 and Equation 37, from the pressure at the inlet of the core. In addition, counters required in the code logic are set equal to 1, denoting the first increment.

The first major calculation in the code is the determination of the bulk temperature rise for the first calculation increment. This is calculated from Equation 48 with \bar{q}_s'' determined from Equation 51. For small calculation increments, the average volumetric thermal source strength can be accurately

approximated by evaluating Equation 1 at $-H/2 + \Delta L/2$; i.e., at the center of the increment.

The average bulk temperature, \bar{T}_B , for the increment is taken as the arithmetic average of the inlet and exit values. All coolant properties used in the pressure drop and heat transfer coefficient calculations are assumed to be functions of temperature only and are evaluated at the average bulk temperature.

Both the friction factor and heat transfer coefficient calculations require the Reynolds number of the flow which is calculated from Equation 33. Then f_{circ} is calculated from Equation 34. To this value the multiplicative correction factors given by Equations 35 and 36 are applied to yield f for the actual reactor flow. Knowing f , the pressure drop for the increment is calculated from Equation 29. The Nusselt number is calculated from Equation 42 and the heat transfer coefficient is then backed out of the Nu definition, Equation 39.

The average outer surface temperature of the cladding for the increment is determined from Newton's law of cooling with \bar{q}_s'' , \bar{T}_B and h available from previous calculations for the increment; i.e.,

$$\bar{T}_s = \bar{T}_B + \frac{\bar{q}_s''}{h} . \quad (53)$$

At this point, the code checks whether boiling is present in the increment. If boiling is observed an informative message is printed and the calculations are terminated.

After the coolant channel calculations for the increment have been performed, the radial temperature distribution in the fuel is calculated for the increment.

First the temperature at the outer surface of the fuel is found. In the fuel rod model, the outer surface of the fuel is at the same temperature as the inner surface of the cladding; therefore the outer surface fuel temperature, \bar{T}_f , can be obtained by adding the temperature drop across the cladding to the outer surface temperature of the cladding, \bar{T}_s , which was calculated earlier.

The temperature drop across the cladding is obtained from Equation 25. In Equation 25 the thermal conductivity of the cladding appears. This property is temperature dependent and should be evaluated at the mean temperature of the cladding. However the mean cladding temperature is dependent on the temperature rise across the cladding. Thus, an iterative-type of solution is called for. The procedure used is to evaluate k_{c-I} at \bar{T}_s , calculate \bar{T}_f , calculate $\bar{T}_{clad\ mean}$, evaluate k_{c-II} at $\bar{T}_{clad\ mean}$, compare k_{c-II} to k_{c-I} . If k_{c-II} is within 1% of k_{c-I} , accept value of \bar{T}_f . If k_{c-II} is not within 1% of k_{c-I} , let $k_{c-I} = k_{c-II}$ and repeat the sequence. In this way, a cladding thermal conductivity accurate to within 1% is obtained.

The next step is to calculate the temperature at the center of the fuel from Equation 17. Again a temperature dependent thermal conductivity, k_f , appears, and an iterative calculation procedure like that described in the previous paragraph is used. The fuel temperatures at the quarter, half, and three-quarter radii are then calculated from Equation 15.

After the calculations for the first increment are completed the results are printed out. Discussion of the output is deferred until Section 5.3. It should be noted here, however, that in the output tabulation the temperatures are reported as having occurred at the axial center of the increment. In other words, for the first increment the results are reported at

$Z = -H/2 + \Delta L/2$. After the results for the first increment have been printed out the code increments to the next segment, and continues this process until all 100 segments have been spanned.

After the completion of the calculations and printout for the 100 segments of the core, the core exit conditions are calculated. This requires a calculation of the exit pressure loss using Equations 29 and 37. Then P_{ex} and T_{ex} are computed and printed, ending the computations.

5.1 Nomenclature

<u>Analysis Symbol</u>	<u>Code Symbol</u>	<u>Description</u>
A		Area
A_f	AFL	Flow area of coolant channel
A_n		Heat transfer area normal to n-direction
A_r		Heat transfer area at radius r
A_s		Heat transfer area at outside of cladding
C_1, C_2, C_3, C_4		Integration constants
C_p	CP	Constant pressure specific heat
D		Diameter
D_e	DEQ	Equivalent diameter of coolant channel
D_f	DFU	Outside diameter of nuclear fuel
D_s	DCL	Outside diameter of cladding
D_{ww}	DWW	Wire wrap diameter
	DR	Ratio of wire wrap diameter to equivalent diameter
E_f		Energy release per fission
e	ERR	Error ratio
f	F	Friction factor
f_o / f_{circ}	FRAT	Ratio of unwrapped fuel bundle to circular tube friction factor
f_{circ}	FCIRC	Friction factor for circular tubes
f / f_o	FWWM	Ratio of actual to unwrapped fuel bundle friction factor
ξ_c		Dimensional constant = $32.174 \frac{\text{lbm-ft}}{\text{sec}^2\text{-lbf}}$

<u>Analysis Symbol</u>	<u>Code Symbol</u>	<u>Description</u>
G	GIN	Mass velocity
h	HTC	Convective heat transfer coefficient
H	H	Height of active core
H_e	HE	Extrapolated height of core
HP	HP	Helical wire wrap pitch
i	ENTH	Enthalpy
i_{in}		Enthalpy at inlet of core
k		Thermal conductivity
k_B	KBC	Thermal conductivity of the coolant
k_c	KCL	Thermal conductivity of cladding
k_{c-I}	KCL1	Thermal conductivity of cladding - at pre-iteration average cladding temperature
k_{c-II}	KCL2	Thermal conductivity of cladding - at updated average cladding temperature
k_f	KFU	Thermal conductivity of fuel
	KFU1	Thermal conductivity of fuel - at pre-iteration average fuel temperature
	KFU2	Thermal conductivity of fuel - at updated average fuel temperature
K		Flow resistance coefficient
L_e		Extrapolation length
ΔL	DELL	Length increment
\dot{m}	MDOT	Mass flow rate
N_{ff}		Number of fissionable fuel nuclei per unit volume
Nu	NU	Nusselt number
Option	$\emptyset P$	Option = 1 for cosine, Option = 2 for coupled program

<u>Analysis Symbol</u>	<u>Code Symbol</u>	<u>Description</u>
P_w	PW	Wetted perimeter
P	PAV	Pressure
P_1	P1	Pressure at beginning of increment
P_2	P2	Pressure at end of increment
P_{ex}	PEX	Core exit pressure
P_{in}	PIN	Core inlet pressure
Pe	PE	Peclet number
Pr	PR	Prandtl number
ΔP		Pressure drop
ΔP_E	DELPE	Exit or entrance pressure loss
ΔP_F	DELPF	Frictional pressure loss
q		Heat transfer rate
q_f		Heat transfer rate at D_f
q_n		Heat transfer rate in n-direction
q_s		Heat transfer rate at D_s
q_s''	SHFAV	Heat flux at D_s
q'''	QTPAV	Volumetric thermal source strength
q_o''	QTPO	Volumetric thermal source strength at center of core
r		Fuel pin radial coordinate
r_f		Radius of fuel
r_s		Outer radius of cladding
R		Core radial coordinate
Re	RE	Reynolds number
S	S	Center-to-center spacing between fuel rods

<u>Analysis Symbol</u>	<u>Code Symbol</u>	<u>Description</u>
S/D_s	SRAT	Ratio of fuel rod spacing to fuel rod diameter
T	T	Temperature
T_o	TO	Temperature at center of fuel rod
$T_{1/4}$	T14	Temperature in fuel at $r = 1/4 r_f$
$T_{1/2}$	T12	Temperature in fuel at $r = 1/2 r_f$
$T_{3/4}$	T34	Temperature in fuel at $r = 3/4 r_f$
T_B	TBAV	Coolant bulk temperature
T_{B1}	TB1	Bulk temperature at beginning of increment
T_{B2}	TB2	Bulk temperature at end of increment
T_f	TF	Temperature in fuel at D_f
T_{ex}	TEX	Core exit temperature
T_{in}	TIN	Core inlet temperature
T_s	TSAV	Cladding surface temperature
T_{sat}	TSATAV	Saturation temperature
T_w		Wall temperature
U		Velocity
U_B	UB	Average velocity in flow channel
X_n		Coordinate in n-direction
Z		Axial coordinate
Z_c	ZC	Axial location of center of increment
Z_m		Axial location of maximum cladding surface temperature
ϵ		Roughness size
θ		Angular coordinate

<u>Analysis Symbol</u>	<u>Code Symbol</u>	<u>Description</u>
μ	VIS	Absolute viscosity
ν		Kinematic viscosity
ρ	RH \emptyset	Density
$\bar{\sigma}_f$		Average fission microscopic cross section
T		Time
ϕ		Neutron flux
superscript -		Average for calculation increment

5.2 Code Input

The input to the LMFBR Thermal-Hydraulics Code is intentionally extremely simple. Only three cards are required; the first lists the geometrical quantities, the second lists the coolant inlet conditions, and the third lists the parameters that describe the volumetric thermal source strength distribution in the reactor.

The required input data cards are listed below. The units of each parameter and their input format are included. Sample input data cards are shown in Figure 2.

Card 1 -- Geometry

D_f (in.)	F 10.4
D_s (in.)	F 10.4
S (in.)	F 10.4
HP (in.)	F 10.2
H (in.)	F 10.1

Card 2 -- Coolant inlet conditions

G (lbm/hr-ft ²)	E 10.3
T_{in} (F)	F 10.1
P_{in} (psia)	F 10.1

Card 3 -- Power distribution

q'''_o (Btu/hr-ft ³)	E 10.3
H_e (in.)	F 10.1
Option (pure number)	I 10

On Card 3 the axial volumetric thermal source strength distribution through the core is specified. For independent operation of the code (Option = 1) a cosine distribution is built into the code and q'''_o and H_e

are the parameters which indicate its level and period. When the LMFBR Thermal-Hydraulics Code is coupled with other codes (Option = 2) the cosine distribution is over-ridden by the actual power distribution which is supplied by the main program.

5.3 Code Output

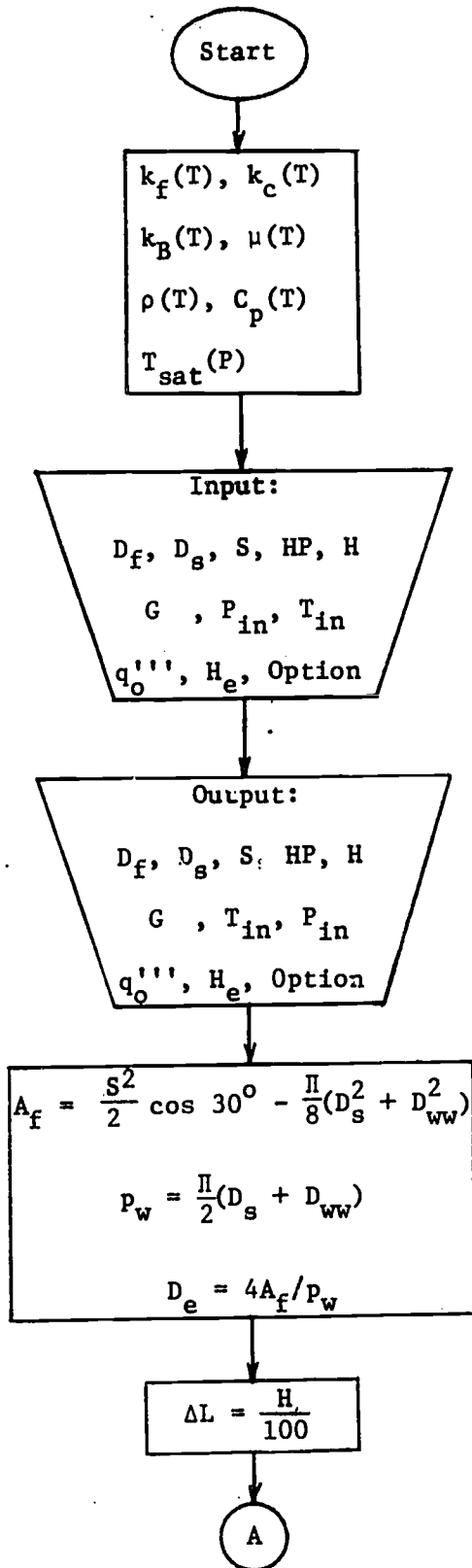
Three sets of information are printed out. Each is printed under completely explicit headings such that there should be no interpretation difficulties.

The first set of output information consists of a listing of the input that was supplied to the code.

The second and main set of output is a tabulation of the temperatures, h , and ΔP for each increment in the core. The temperature printed out are \bar{T}_0 , $\bar{T}_{1/4}$, $\bar{T}_{1/2}$, $\bar{T}_{3/4}$, \bar{T}_f , \bar{T}_s , \bar{T}_B , \bar{T}_{sat} . From this data, observations of the maximum fuel and cladding temperatures and their locations can be made.

The third set of data reports the core exit pressure and temperature.

5.4 Code Flow Chart



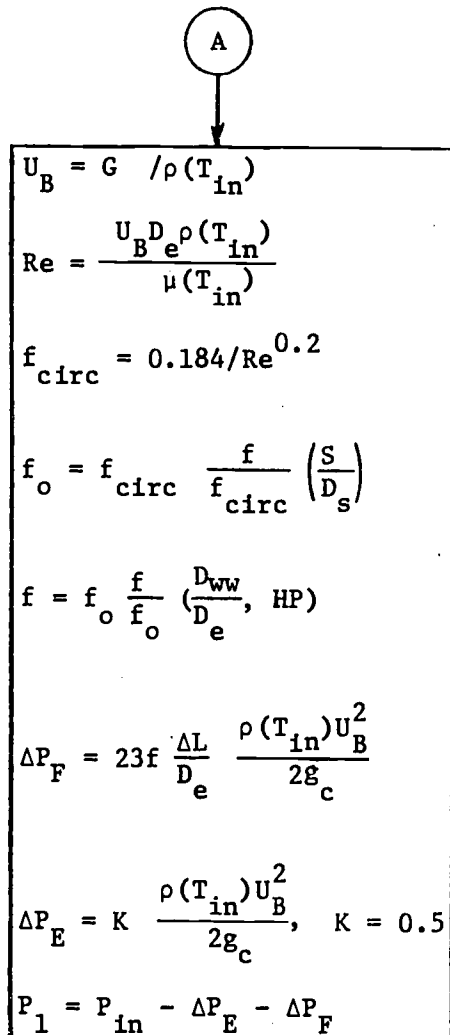
Functional relations between variables supplied to code as polynomials.

Geometry, inlet coolant conditions, and power distribution supplied to code.

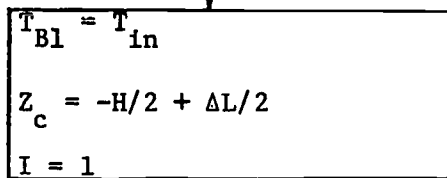
Printout of geometry, inlet coolant conditions, and power distribution.

Calculation of flow channel geometrical parameters.

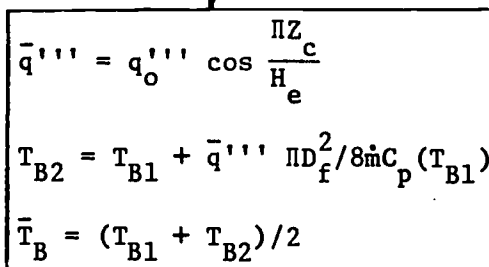
Selection of calculation increment.



Calculation of permanent pressure loss at inlet and resulting pressure at start of active core.



Initializing temperature, position, and increment counter for 1st increment.



Calculation of average bulk temperature of coolant for increment.



C

$$U_B = G / \rho(\bar{T}_B)$$

$$Re = \frac{U_B D_e \rho(\bar{T}_B)}{\mu(\bar{T}_B)}$$

$$f_{\text{circ}} = 0.184 / Re^{0.2}$$

$$f_o = f_{\text{circ}} \frac{f(S)}{f_{\text{circ}}(D_s)}$$

$$f = f_o \frac{f}{f_o} \left(\frac{D_{ww}}{D_e}, \text{HP} \right)$$

$$\Delta P_F = f \frac{\Delta L}{D_e} \frac{\rho(\bar{T}_B) U_B^2}{2g_c}$$

$$P_2 = P_1 - \Delta P_F$$

$$\bar{P} = (P_1 + P_2) / 2$$

$$\bar{T}_{\text{sat}} = T_{\text{sat}}(\bar{P})$$

Calculation of pressure drop and average saturation temperature for increment.

↓

$$Pr = \frac{C_p(\bar{T}_B) \mu(\bar{T}_B)}{k_B(\bar{T}_B)}$$

$$Pe = RePr$$

$$Nu = Nu(Pe, \frac{S}{D_s})$$

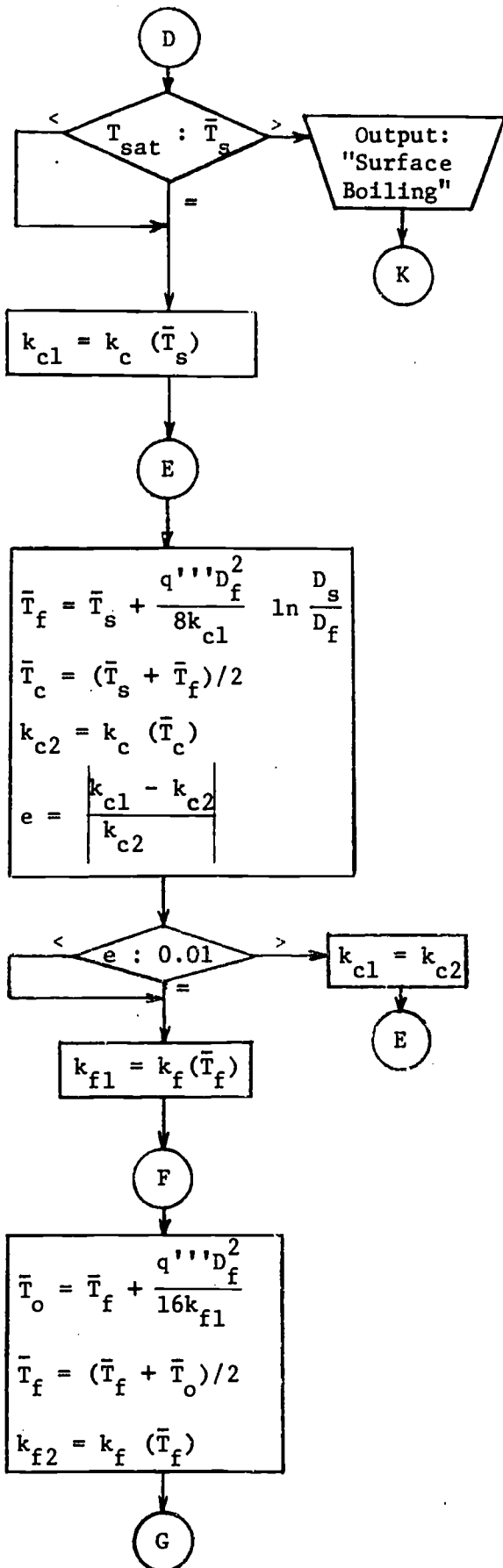
$$h = \frac{Nu k_B(\bar{T}_B)}{D_e}$$

$$\bar{T}_s = T_B + \frac{\bar{q}'' D_s^2}{4 D_s h}$$

Calculation of heat transfer coefficient and average cladding surface temperature for increment.

↓

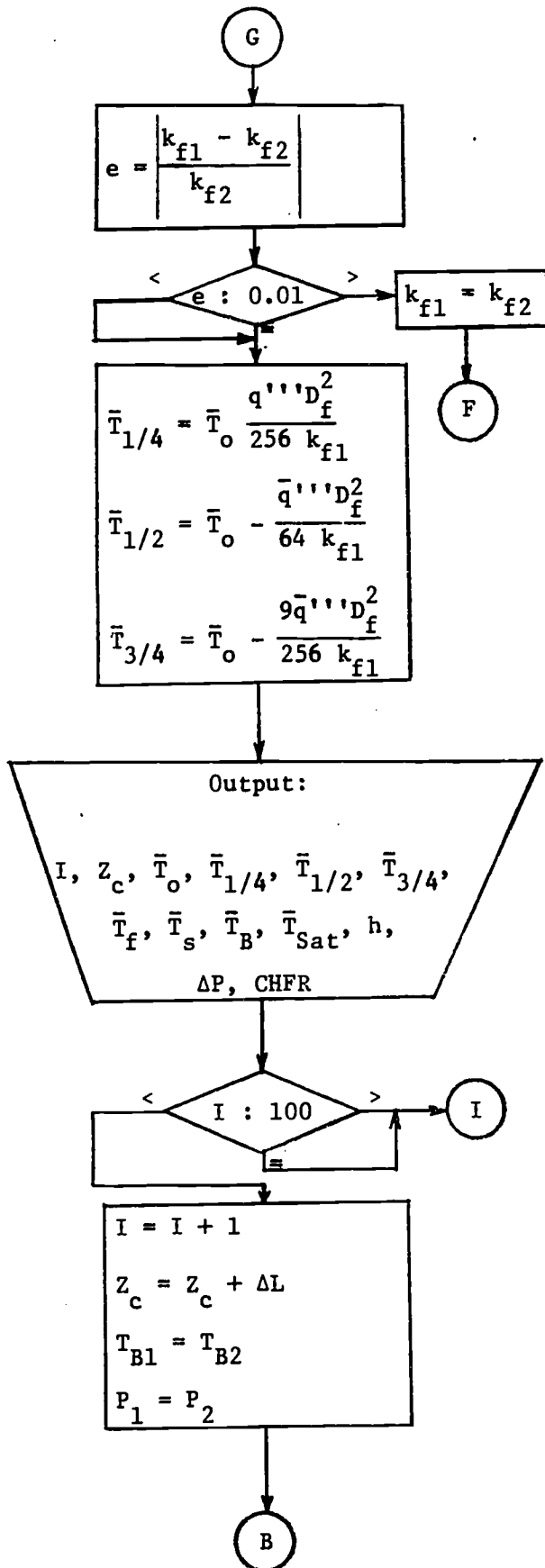
D



Check to see if subcooled boiling is possible. If possibility is detected, a message is printed and calculations are terminated. If no boiling is indicated, program proceeds to calculation of fuel and cladding temperatures.

Calculation of temperature rise across cladding. The thermal conductivity of the cladding is evaluated at the mean cladding temperature by an iterative technique.

Calculation of fuel centerline temperature. The thermal conductivity of the fuel is evaluated at a mean fuel temperature by an iterative technique.

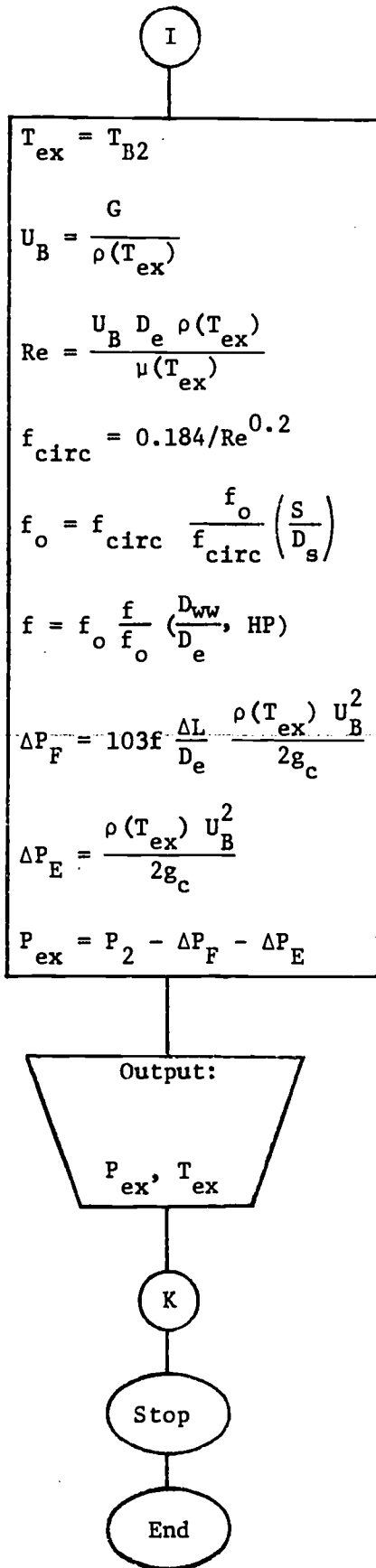


Evaluation of fuel temperature at the quarter, half, and three quarter diameter points.

Printout of thermal-hydraulic parameters for increment.

Check to see if entire core has been calculated.

Initializing for next calculation increment.



Calculation of pressure loss in gas plenum and downstream rod support region.

Printout of coolant core exit conditions.

5.5 Code Examples

The following examples demonstrate the use of the LMFBR Thermal-Hydraulics Code to calculate the thermal-hydraulic behavior of a typical LMFBR.

Example 7.

A LMFBR core is composed of 0.250 in. diameter fuel rods 5 ft long and spaced 0.325 in. in a triangular array. The fuel diameter is 0.220 in. and the wire wrap pitch is 12 in. The liquid sodium inlet conditions are 800 F and 200 psia. The average coolant velocity in the inlet of the core is 28.80 ft/sec. The average fuel rod produces 8.04 kw/ft. Assume an extrapolation length equal to 5% of the core height. Determine the magnitudes and locations of the maximum fuel temperature and the maximum cladding temperature.

Solution.

The mass velocity, extrapolated core height, and peak volumetric thermal source strength must first be computed from the data given.

$$\begin{aligned} G &= \rho U_B = (53.1 \text{ lbm/ft}^3)(28.80 \text{ ft/sec})(3600 \text{ sec/hr}) \\ &= 5.5 \times 10^6 \text{ lbm/hr-ft}^2 \end{aligned}$$

$$\begin{aligned} H_e &= H + 2L_e = H + 2(0.05H) = 1.10H \\ &= 1.10 (5 \text{ ft}) = 5.5 \text{ ft} = 66.0 \text{ in.} \end{aligned}$$

$$q''_o = 2P_{ave} / [H_e D_f^2 \sin(\pi H / 2 H_e)]$$

$$\begin{aligned} &= 2(8.04 \text{ kw/ft})(12 \text{ ft})(3413 \text{ Btu/kw-hr})/\{(5.5 \text{ ft})(0.220 \text{ in.})^2 \\ &\quad (\text{ft}/12 \text{ in.})^2 \sin[\pi(5 \text{ ft})/2(5.5 \text{ ft})]\} \\ &= 1.5 \times 10^8 \text{ Btu/hr-ft}^3. \end{aligned}$$

From the output printout of the code (see next five pages) we find

$$T_{\text{clad max}} = 1120.0 \text{ F at } Z = 1.925 \text{ ft}$$

$$T_{\text{fuel max}} = 3548.2 \text{ F at } Z = 0.025 \text{ ft.}$$

LMFBR THERMAL HYDRAULICS CODE

INPUT DATA

FUEL O.D. (INCH)	CLAD O.D. (INCH)	ROD PITCH (INCH)	ACTIVE CORE LENGTH (INCH)
0.2200	0.2500	0.3250	60.00

WIRE WRAP PITCH
(INCH)
12.00

INLET MASS VELOCITY (LB/HR-FT**2)	CORE INLET TEMPERATURE (F)	CORE INLET PRESSURE (PSIA)
0.550E 07	800.00	200.00

VOLUMETRIC THERMAL SOURCE STRENGTH (BTU/HR-FT**3)	EXTRAPOLATED HEIGHT (INCH)
0.1500E 09	66.00

OPTION 1

END OF INPUT DATA

AT THE INLET OF THE CORE

CHANNEL AVE. VELOCITY (FT/SEC)	REYNOLDS #	FRICTION FACTOR
28.80	111627.4	0.0180

NO	Z-LOC.	T0	T1/4	T1/2	T3/4	TF
	T CLAD	T BULK	T SAT	H T COEFF	DELTA P	
1	-2.475	1129.7	1130.5	1058.1	956.1	813.3
	802.5	800.3	2289.8	44078.8	50.31	
2	-2.425	1212.1	1201.0	1113.2	989.5	816.3
	803.6	801.1	2289.2	44068.6	50.31	
3	-2.375	1288.3	1275.1	1171.1	1024.6	819.5
	804.8	801.9	2288.6	44056.6	50.30	
4	-2.325	1368.3	1353.0	1231.9	1061.4	822.7
	806.2	802.9	2288.0	44042.9	50.30	
5	-2.275	1452.1	1434.5	1295.6	1100.0	826.1
	807.6	803.9	2287.4	44027.6	50.30	
6	-2.225	1541.2	1521.2	1363.3	1140.9	829.5
	809.2	805.1	2286.8	44010.7	50.30	
7	-2.175	1633.1	1610.7	1433.1	1183.1	833.1
	810.9	806.4	2286.2	43992.1	50.29	
8	-2.125	1728.4	1703.4	1505.5	1226.8	836.7
	812.7	807.8	2285.6	43971.9	50.29	
9	-2.075	1826.5	1798.8	1579.9	1271.8	840.4
	814.6	809.4	2285.0	43950.0	50.28	
10	-2.025	1926.3	1895.9	1655.7	1317.6	844.2
	816.6	811.0	2284.4	43926.6	50.28	
11	-1.975	2026.7	1993.6	1732.1	1363.7	848.0
	818.7	812.8	2283.8	43901.7	50.28	
12	-1.925	2126.5	2090.7	1807.9	1409.6	852.0
	820.9	814.7	2283.2	43875.2	50.27	
13	-1.875	2224.3	2185.9	1882.2	1454.7	856.0
	823.3	816.6	2282.6	43847.2	50.27	
14	-1.825	2318.9	2278.0	1954.2	1498.3	860.1
	825.7	818.7	2282.0	43817.6	50.26	
15	-1.775	2406.6	2363.3	2021.0	1539.0	864.3
	828.2	820.9	2281.3	43786.7	50.26	
16	-1.725	2493.4	2447.8	2087.2	1579.4	868.5
	830.9	823.2	2280.7	43754.3	50.25	
17	-1.675	2575.0	2527.2	2149.4	1617.5	872.8
	833.6	825.6	2280.1	43720.4	50.25	
18	-1.625	2651.0	2601.2	2207.5	1653.2	877.1
	836.4	828.1	2279.5	43685.2	50.24	
19	-1.575	2722.1	2670.4	2261.9	1686.8	881.5
	839.3	830.7	2278.9	43648.7	50.23	
20	-1.525	2787.3	2733.9	2312.0	1717.8	886.0
	842.3	833.4	2278.3	43610.8	50.23	
21	-1.475	2848.5	2793.5	2359.0	1747.1	890.5
	845.4	836.2	2277.7	43571.7	50.22	
22	-1.425	2905.8	2849.3	2403.1	1774.7	895.0
	848.6	839.1	2277.0	43531.3	50.21	
23	-1.375	2962.4	2904.5	2446.7	1802.1	899.6
	851.9	842.0	2276.4	43489.7	50.21	

24	-1.325	3011.2	2952.0	2484.4	1826.0	904.2
		855.2	845.1	2275.8	43446.9	50.20
25	-1.275	3056.1	2995.8	2519.3	1848.3	908.9
		858.6	848.2	2275.2	43403.0	50.19
26	-1.225	3098.5	3037.1	2552.2	1869.4	913.5
		862.1	851.5	2274.6	43357.9	50.19
27	-1.175	3142.9	3080.4	2586.7	1891.5	918.2
		865.7	854.8	2273.9	43311.9	50.18
28	-1.125	3182.2	3118.7	2617.4	1911.4	923.0
		869.3	858.1	2273.3	43264.8	50.17
29	-1.075	3213.2	3149.0	2641.8	1927.6	927.7
		873.0	861.6	2272.7	43216.7	50.17
30	-1.025	3249.5	3184.5	2670.3	1946.2	932.5
		876.8	865.1	2272.1	43167.7	50.16
31	-0.975	3281.3	3215.4	2695.3	1962.8	937.3
		880.6	868.7	2271.5	43117.8	50.15
32	-0.925	3306.3	3239.9	2715.3	1976.4	942.1
		884.5	872.4	2270.8	43067.0	50.15
33	-0.875	3332.4	3265.4	2736.0	1990.5	946.8
		888.5	876.1	2270.2	43015.4	50.14
34	-0.825	3361.6	3293.9	2759.1	2006.0	951.6
		892.4	879.9	2269.6	42963.1	50.13
35	-0.775	3381.3	3313.2	2775.1	2017.3	956.4
		896.5	883.7	2268.9	42910.0	50.12
36	-0.725	3402.0	3333.5	2791.8	2029.1	961.2
		900.6	887.6	2268.3	42856.3	50.12
37	-0.675	3425.6	3356.5	2810.7	2042.1	966.0
		904.7	891.6	2267.7	42802.0	50.11
38	-0.625	3444.2	3374.8	2825.9	2052.9	970.7
		908.9	895.6	2267.1	42747.1	50.10
39	-0.575	3456.6	3386.9	2836.3	2061.0	975.5
		913.1	899.6	2266.4	42691.6	50.10
40	-0.525	3471.1	3401.1	2848.4	2070.0	980.2
		917.3	903.7	2265.8	42635.7	50.09
41	-0.475	3489.1	3418.7	2863.0	2080.5	984.9
		921.6	907.9	2265.1	42579.3	50.08
42	-0.425	3501.7	3431.1	2873.7	2088.6	989.6
		925.8	912.0	2264.5	42522.5	50.08
43	-0.375	3508.1	3437.5	2879.6	2094.0	994.2
		930.1	916.2	2263.9	42465.4	50.07
44	-0.325	3517.2	3446.5	2887.6	2100.6	998.8
		934.5	920.5	2263.2	42408.0	50.07
45	-0.275	3529.5	3458.6	2898.0	2108.6	1003.4
		938.8	924.7	2262.6	42350.3	50.06
46	-0.225	3536.6	3465.6	2904.4	2114.2	1007.9
		943.2	929.0	2262.0	42292.5	50.06
47	-0.175	3542.4	3471.3	2909.9	2119.3	1012.4
		947.5	933.3	2261.3	42234.4	50.05
48	-0.125	3542.7	3471.8	2911.2	2121.9	1016.8
		951.9	937.6	2260.7	42176.3	50.04
49	-0.075	3545.7	3474.8	2914.6	2125.7	1021.2
		956.2	941.9	2260.0	42118.2	50.04
50	-0.025	3547.6	3476.7	2917.0	2128.9	1025.5
		960.6	946.2	2259.4	42060.0	50.04

51	0.025	3548.2	3477.5	2918.6	2131.6	1029.8
	964.9	950.5	2258.8	42001.9	50.03	
52	0.075	3547.7	3477.1	2919.3	2133.7	1034.0
	969.3	954.9	2258.1	41943.9	50.03	
53	0.125	3546.1	3475.6	2919.1	2135.3	1038.1
	973.6	959.2	2257.5	41886.0	50.02	
54	0.175	3543.2	3473.0	2918.0	2136.4	1042.2
	977.9	963.5	2256.8	41828.3	50.02	
55	0.225	3543.1	3473.0	2918.9	2138.6	1046.2
	982.2	967.8	2256.2	41770.8	50.02	
56	0.275	3537.6	3467.7	2915.7	2138.4	1050.1
	986.5	972.1	2255.5	41713.6	50.01	
57	0.325	3530.9	3461.3	2911.7	2137.6	1053.9
	990.7	976.4	2254.9	41656.7	50.01	
58	0.375	3519.0	3449.9	2903.7	2134.5	1057.7
	994.9	980.7	2254.2	41600.2	50.01	
59	0.425	3510.4	3441.6	2898.1	2132.8	1061.4
	999.1	984.9	2253.6	41544.1	50.01	
60	0.475	3500.5	3432.1	2891.6	2130.5	1064.9
	1003.2	989.1	2252.9	41488.5	50.00	
61	0.525	3492.9	3424.8	2886.8	2129.2	1068.4
	1007.3	993.3	2252.2	41433.4	50.00	
62	0.575	3479.9	3412.3	2877.9	2125.4	1071.8
	1011.3	997.5	2251.6	41378.8	50.00	
63	0.625	3462.0	3395.0	2865.3	2119.4	1075.1
	1015.3	1001.6	2250.9	41324.8	50.00	
64	0.675	3447.2	3380.6	2855.0	2114.7	1078.4
	1019.2	1005.6	2250.3	41271.5	50.00	
65	0.725	3434.6	3368.5	2846.3	2110.9	1081.5
	1023.1	1009.7	2249.6	41218.8	50.00	
66	0.775	3416.2	3350.7	2833.2	2104.6	1084.5
	1026.9	1013.6	2249.0	41166.8	50.00	
67	0.825	3392.8	3328.1	2816.4	2096.0	1087.3
	1030.7	1017.6	2248.3	41115.6	50.00	
68	0.875	3372.5	3308.4	2801.9	2088.7	1090.1
	1034.3	1021.4	2247.6	41065.2	50.00	
69	0.925	3354.2	3290.7	2788.9	2082.2	1092.8
	1038.0	1025.2	2247.0	41015.6	50.00	
70	0.975	3329.9	3267.1	2771.2	2073.0	1095.4
	1041.5	1029.0	2246.3	40966.9	50.00	
71	1.025	3300.4	3238.5	2749.7	2061.4	1097.8
	1045.0	1032.7	2245.6	40919.2	50.00	
72	1.075	3273.9	3212.8	2730.5	2051.2	1100.1
	1048.4	1036.3	2245.0	40872.3	50.00	
73	1.125	3245.6	3185.4	2709.8	2040.0	1102.3
	1051.7	1039.8	2244.3	40826.4	50.00	
74	1.175	3218.1	3158.7	2689.7	2029.2	1104.4
	1054.9	1043.3	2243.6	40781.6	50.00	
75	1.225	3185.1	3126.7	2665.4	2015.8	1106.4
	1058.1	1046.7	2243.0	40737.8	50.01	
76	1.275	3147.4	3090.2	2637.6	2000.4	1108.2
	1061.1	1050.0	2242.3	40695.1	50.01	
77	1.325	3111.6	3055.3	2611.2	1985.6	1109.9
	1064.1	1053.2	2241.6	40653.5	50.01	

78	1.375	3076.5	3021.3	2585.3	1971.2	1111.5
	1066.9	1056.4	2240.9	40613.1	50.01	
79	1.425	3034.8	2980.8	2554.3	1953.8	1113.0
	1069.7	1059.5	2240.3	40573.8	50.01	
80	1.475	2990.8	2933.1	2521.7	1935.3	1114.3
	1072.4	1062.4	2239.6	40535.7	50.02	
81	1.525	2942.0	2890.7	2485.4	1914.6	1115.5
	1074.9	1065.3	2238.9	40498.9	50.02	
82	1.575	2894.0	2844.1	2449.7	1894.2	1116.5
	1077.4	1068.1	2238.0	40463.3	50.02	
83	1.625	2846.0	2797.4	2413.9	1873.7	1117.4
	1079.8	1070.8	2237.5	40429.0	50.02	
84	1.675	2790.1	2743.2	2372.2	1849.7	1118.2
	1082.0	1073.4	2236.9	40396.0	50.03	
85	1.725	2731.5	2686.2	2328.3	1824.4	1118.9
	1084.1	1075.9	2236.2	40364.4	50.03	
86	1.775	2668.0	2624.5	2280.8	1796.9	1119.4
	1086.2	1078.2	2235.5	40334.0	50.03	
87	1.825	2606.9	2565.2	2235.1	1770.4	1119.7
	1088.1	1080.5	2234.8	40305.2	50.03	
88	1.875	2536.4	2496.6	2182.3	1739.7	1120.0
	1089.9	1082.7	2234.1	40277.6	50.04	
89	1.925	2464.0	2426.2	2128.0	1708.0	1120.0
	1091.6	1084.7	2233.4	40251.5	50.04	
90	1.975	2387.3	2351.7	2070.5	1674.5	1120.0
	1093.1	1086.7	2232.7	40226.9	50.04	
91	2.025	2306.9	2273.5	2010.1	1639.1	1119.8
	1094.6	1088.5	2232.1	40203.7	50.04	
92	2.075	2223.1	2192.1	1947.2	1602.3	1119.5
	1095.9	1090.2	2231.4	40181.9	50.05	
93	2.125	2139.1	2110.5	1884.1	1565.3	1119.0
	1097.1	1091.8	2230.7	40161.7	50.05	
94	2.175	2050.9	2024.7	1817.2	1526.4	1118.4
	1098.2	1093.3	2230.0	40143.0	50.05	
95	2.225	1961.2	1937.5	1750.3	1486.7	1117.7
	1099.1	1094.7	2229.3	40125.8	50.05	
96	2.275	1870.8	1849.6	1682.3	1446.6	1116.8
	1100.0	1095.9	2228.6	40110.0	50.05	
97	2.325	1780.6	1761.9	1614.4	1406.6	1115.8
	1100.7	1097.1	2227.9	40095.9	50.06	
98	2.375	1691.3	1675.1	1547.1	1366.9	1114.6
	1101.3	1098.1	2227.2	40083.3	50.06	
99	2.425	1603.8	1590.0	1481.2	1327.9	1113.3
	1101.7	1098.9	2226.5	40072.2	50.06	
100	2.475	1518.0	1506.6	1416.5	1289.6	1111.9
	1102.0	1099.7	2225.8	40062.7	50.06	

EXIT PRESSURE

EXIT TEMPERATURE

114.0

1100.0

POWER PER UNIT LENGTH (KW/FT)

8.04

Example 8.

The effect of oversized cladding on LMFBR thermal-hydraulic performance is to be studied. Consider the LMFBR described in Example 7 but with an outer cladding diameter of 0.275 in. (instead of 0.250 in.). Compare the following thermal-hydraulic parameters for the "oversized cladding" and "normal" flow channels:

- a. Location and magnitude of maximum fuel temperature
- b. Location and magnitude of maximum cladding temperature
- c. Exit sodium temperature.

Solution.

Each flow channel in the fuel assembly will experience the same pressure drop. The "oversized cladding" flow channel will have a smaller equivalent diameter and hence will pass less flow for the same pressure loss (as shown in Example 5). To assure approximately the same pressure loss as in the "normal" channels the mass velocity of the "oversized cladding" channel must be adjusted. The equivalent diameters are computed first.

"Normal" channel:

$$\begin{aligned} A_f &= \frac{1}{2} S^2 \cos 30^\circ = \frac{\pi}{8} (D_s^2 + D_{ww}^2) \\ &= 1/2(0.325)^2 \cos 30^\circ - \frac{\pi}{8} [(0.250)^2 + (0.075)^2] \\ &= 0.0191 \text{ in.}^2 \end{aligned}$$

$$\begin{aligned} p_w &= \frac{\pi}{2} (D_s + D_{ww}) = \frac{\pi}{2} (0.250 + 0.075) \\ &= 0.511 \text{ in.} \end{aligned}$$

$$D_e = 4 A_f / p_w$$

$$= 4(0.0150)/0.511$$

$$= 0.1497 \text{ in.}$$

"Oversized cladding" channel:

$$A_f = \frac{1}{2} S^2 \cos 30^\circ - \frac{\pi}{8} (D_s^2 + D_{ww}^2)$$

$$= 1/2(0.325)^2 \cos 30^\circ - \frac{\pi}{8} [(0.275)^2 + (0.050)^2]$$

$$= 0.0150 \text{ in.}^2$$

$$P_w = \frac{\pi}{2} (D_s + D_{ww}) = \frac{\pi}{2} (0.275 + 0.050)$$

$$= 0.511 \text{ in.}$$

$$D_e = 4 A_f / P_w$$

$$= 4(0.0150)/0.511$$

$$= 0.1173 \text{ in.}$$

From the results of Example 5,

$$G_{oc} = G_N (D_{eoc} / D_{eN})^{2/3}$$

$$= 5.50 \times 10^6 (0.1173/0.1497)^{2/3}$$

$$= 4.69 \times 10^6 \text{ lbm/hr-ft}^2.$$

The input to the LMFBR Thermal-Hydraulics Code is the same as that for Example 7 except for the new value of G computed above and the oversized D_s . From the code (printout next five pages) the following results are obtained:

LMFBR THERMAL HYDRAULICS CODE

INPUT DATA

FUEL O.D. (INCH)	CLAD O.D. (INCH)	ROD PITCH (INCH)	ACTIVE CORE LENGTH (INCH)
0.2200	0.2750	0.3250	60.00

WIRE WRAP PITCH
(INCH)
12.00

INLET MASS VELOCITY (LB/HR-FT**2)	CORE INLET TEMPERATURE (F)	CORE INLET PRESSURE (PSIA)
0.4690E 07	800.00	200.00

VOLUMETRIC THERMAL SOURCE STRENGTH (BTU/HR-FT**3)	EXTRAPOLATED HEIGHT (INCH)
0.1500E 09	66.00

OPTION 1

END OF INPUT DATA

AT THE INLET OF THE CORE

CHANNEL AVE. VELOCITY (FT/SEC)	REYNOLDS #	FRICTION FACTOR
24.56	75497.9	0.0195

NO	Z-LOC.	TO	T1/4	T1/2	T3/4	TF
	T CLAD	T HULK	T SAT	H T COEF	DELTA P	
1	-2.475	1150.3	1141.0	1068.1	965.4	821.6
	802.8	800.5	2290.6	38036.8	51.59	
2	-2.425	1225.6	1214.4	1125.8	1001.1	826.4
	804.2	801.6	2289.9	38024.1	51.59	
3	-2.375	1305.0	1291.7	1186.6	1038.6	831.4
	805.9	802.8	2289.3	38009.4	51.59	
4	-2.325	1388.5	1373.0	1250.5	1078.0	836.6
	807.7	804.2	2288.7	37992.7	51.58	
5	-2.275	1476.1	1458.2	1317.5	1119.3	841.8
	809.7	805.8	2288.1	37973.8	51.58	
6	-2.225	1569.1	1548.8	1388.6	1163.0	847.2
	811.9	807.6	2287.5	37953.0	51.57	
7	-2.175	1665.1	1642.3	1462.0	1208.2	852.8
	814.2	809.5	2286.9	37930.1	51.57	
8	-2.125	1764.4	1739.0	1537.9	1254.8	858.4
	816.7	811.6	2286.2	37905.3	51.56	
9	-2.075	1866.2	1838.0	1615.7	1302.5	864.2
	819.3	813.9	2285.6	37878.5	51.56	
10	-2.025	1969.2	1938.3	1694.4	1350.9	870.1
	822.2	816.3	2285.0	37849.8	51.55	
11	-1.975	2072.2	2038.6	1773.2	1399.4	876.1
	825.2	818.9	2284.4	37819.1	51.55	
12	-1.925	2173.7	2137.4	1850.8	1447.2	882.2
	828.3	821.7	2283.8	37786.6	51.54	
13	-1.875	2272.2	2233.3	1926.2	1493.8	888.4
	831.6	824.6	2283.1	37752.2	51.53	
14	-1.825	2364.5	2323.2	1997.0	1537.7	894.7
	835.0	827.7	2282.5	37716.0	51.52	
15	-1.775	2455.1	2411.4	2066.6	1580.9	900.1
	838.7	831.0	2281.9	37678.0	51.52	
16	-1.725	2540.3	2494.4	2132.1	1621.9	907.5
	842.4	834.4	2281.3	37638.3	51.51	
17	-1.675	2616.8	2569.0	2191.2	1659.0	914.1
	846.3	837.9	2280.6	37596.8	51.50	
18	-1.625	2694.8	2645.0	2251.3	1696.9	920.7
	850.4	841.6	2280.0	37553.6	51.49	
19	-1.575	2762.2	2710.7	2303.5	1730.2	927.4
	854.6	845.5	2279.4	37508.9	51.48	
20	-1.525	2826.3	2773.2	2353.3	1762.0	934.2
	858.9	849.4	2278.8	37462.5	51.47	
21	-1.475	2887.9	2833.2	2401.2	1792.6	941.1
	863.4	853.6	2278.1	37414.6	51.46	
22	-1.425	2943.4	2887.3	2444.5	1820.9	947.9
	868.0	857.8	2277.5	37365.2	51.46	
23	-1.375	2997.5	2940.1	2486.8	1848.5	954.9
	872.7	862.2	2276.9	37314.3	51.45	

24	-1.325	3041.3	2982.9	2521.4	1871.6	961.9
		877.5	866.8	2276.2	37262.0	51.44
25	-1.275	3089.7	3030.1	2559.5	1896.7	968.9
		882.5	871.4	2275.6	37208.3	51.43
26	-1.225	3133.1	3072.5	2593.8	1919.7	976.0
		887.5	876.2	2275.0	37153.3	51.42
27	-1.175	3168.7	3107.3	2622.3	1939.3	983.1
		892.7	881.1	2274.3	37097.0	51.41
28	-1.125	3204.6	3142.4	2651.0	1959.0	990.2
		898.0	886.1	2273.7	37039.5	51.40
29	-1.075	3243.5	3180.4	2681.9	1980.0	997.3
		903.4	891.3	2273.0	36980.9	51.39
30	-1.025	3272.3	3208.6	2705.4	1996.7	1004.5
		908.9	896.5	2272.4	36921.1	51.38
31	-0.975	3301.8	3237.3	2729.1	2013.5	1011.7
		914.5	901.9	2271.8	36860.3	51.37
32	-0.925	3333.4	3268.3	2754.7	2031.4	1018.8
		920.2	907.3	2271.1	36798.5	51.36
33	-0.875	3380.1	3294.5	2776.5	2047.1	1026.0
		926.0	912.9	2270.5	36735.7	51.36
34	-0.825	3379.9	3314.0	2793.2	2059.8	1033.2
		931.9	918.5	2269.8	36672.0	51.35
35	-0.775	3405.8	3339.3	2814.4	2075.2	1040.3
		937.8	924.2	2269.2	36607.5	51.34
36	-0.725	3427.0	3360.1	2832.1	2088.5	1047.5
		943.8	930.0	2268.6	36542.3	51.33
37	-0.675	3442.3	3375.2	2845.3	2099.2	1054.6
		949.9	935.9	2267.9	36476.3	51.33
38	-0.625	3459.4	3392.0	2859.9	2110.7	1061.7
		956.0	941.9	2267.3	36409.6	51.32
39	-0.575	3479.3	3411.6	2876.7	2123.4	1068.7
		962.2	947.9	2266.6	36342.3	51.31
40	-0.525	3494.3	3426.4	2889.7	2133.9	1075.7
		968.5	954.0	2266.0	36274.5	51.31
41	-0.475	3503.7	3435.7	2898.4	2141.9	1082.7
		974.8	960.1	2265.3	36206.2	51.30
42	-0.425	3515.3	3447.2	2908.9	2150.9	1089.7
		981.1	966.3	2264.7	36137.4	51.30
43	-0.375	3525.7	3457.4	2918.4	2159.3	1096.5
		987.5	972.6	2264.0	36068.4	51.29
44	-0.325	3538.6	3470.2	2929.8	2168.8	1103.4
		993.9	978.9	2263.4	35999.0	51.29
45	-0.275	3546.7	3478.2	2937.5	2176.1	1110.1
		1000.3	985.2	2262.7	35929.3	51.28
46	-0.225	3553.4	3485.0	2944.3	2182.8	1116.8
		1006.8	991.6	2262.1	35859.5	51.28
47	-0.175	3558.9	3490.5	2950.0	2189.0	1123.5
		1013.3	998.0	2261.4	35789.5	51.28
48	-0.125	3559.6	3491.4	2952.2	2193.0	1130.0
		1019.8	1004.4	2260.7	35719.5	51.28
49	-0.075	3563.0	3494.8	2956.3	2198.1	1136.5
		1026.3	1010.9	2260.1	35649.4	51.28
50	-0.025	3568.9	3500.8	2962.4	2204.2	1142.8
		1032.8	1017.3	2259.4	35579.4	51.28

51	0.025	3569.4	3501.4	2964.3	2208.0	1149.1
		1039.3	1023.8	2258.8	35509.5	51.28
52	0.075	3565.6	3497.9	2963.0	2209.8	1155.3
		1045.8	1030.3	2258.1	35439.8	51.28
53	0.125	3567.8	3500.2	2966.2	2214.2	1161.4
		1052.2	1036.7	2257.4	35370.2	51.28
54	0.175	3565.5	3498.2	2966.0	2216.6	1167.4
		1058.7	1043.2	2256.8	35301.0	51.28
55	0.225	3561.9	3494.8	2964.7	2218.3	1173.2
		1065.1	1049.6	2256.1	35232.1	51.29
56	0.275	3553.5	3486.8	2959.8	2217.8	1179.0
		1071.5	1056.1	2255.4	35163.6	51.29
57	0.325	3551.0	3484.5	2959.4	2219.9	1184.6
		1077.9	1062.5	2254.8	35095.5	51.29
58	0.375	3543.9	3477.8	2955.5	2219.9	1190.1
		1084.2	1068.8	2254.1	35027.9	51.30
59	0.425	3532.1	3466.5	2948.0	2217.8	1195.5
		1090.4	1075.2	2253.4	34960.8	51.31
60	0.475	3526.4	3461.1	2945.0	2218.3	1200.8
		1096.7	1081.5	2252.8	34894.4	51.31
61	0.525	3516.1	3451.2	2938.6	2216.6	1205.9
		1102.8	1087.7	2252.1	34828.6	51.32
62	0.575	3504.5	3440.1	2931.1	2214.3	1210.9
		1108.9	1093.9	2251.4	34763.6	51.33
63	0.625	3491.6	3427.7	2922.7	2211.4	1215.7
		1114.9	1100.1	2250.7	34699.3	51.34
64	0.675	3477.5	3414.1	2913.2	2207.9	1220.4
		1120.9	1106.2	2250.1	34635.8	51.35
65	0.725	3458.9	3396.2	2900.4	2202.3	1224.9
		1126.7	1112.2	2249.4	34573.1	51.36
66	0.775	3442.9	3380.7	2889.5	2197.7	1229.3
		1132.5	1118.1	2248.7	34511.4	51.37
67	0.825	3428.3	3366.6	2879.6	2193.7	1233.5
		1138.2	1124.0	2248.0	34450.6	51.38
68	0.875	3406.0	3345.1	2863.9	2186.2	1237.5
		1143.8	1129.8	2247.3	34390.8	51.39
69	0.925	3388.7	3328.4	2851.9	2180.8	1241.4
		1149.3	1135.5	2246.7	34332.0	51.41
70	0.975	3367.0	3307.4	2836.5	2173.4	1245.1
		1154.7	1141.1	2246.0	34274.3	51.42
71	1.025	3344.0	3285.1	2820.2	2165.4	1248.6
		1160.0	1146.6	2245.3	34217.8	51.43
72	1.075	3316.2	3258.2	2800.2	2155.1	1252.0
		1165.2	1152.1	2244.6	34162.4	51.45
73	1.125	3293.5	3236.2	2783.9	2146.9	1255.2
		1170.3	1157.4	2243.9	34108.2	51.46
74	1.175	3266.1	3209.7	2764.1	2136.6	1258.2
		1175.2	1162.6	2243.2	34055.2	51.48
75	1.225	3257.0	3181.5	2743.0	2125.5	1261.0
		1180.0	1167.7	2242.5	34003.5	51.49
76	1.275	3206.1	3151.5	2720.5	2113.4	1263.6
		1184.7	1172.6	2241.8	33953.2	51.51
77	1.325	3173.3	3119.7	2696.5	2100.4	1266.0
		1189.3	1177.5	2241.1	33904.2	51.52

78	1.375	3138.5	3086.0	2671.0	2086.5	1268.3
	1193.7	1182.2	2240.5	33856.5	51.54	
79	1.425	3101.8	3050.3	2643.9	2071.6	1270.3
	1198.0	1186.8	2239.8	33810.4	51.55	
80	1.475	3062.9	3012.6	2615.2	2055.6	1272.2
	1202.1	1191.3	2239.1	33765.6	51.57	
81	1.525	3021.9	2972.8	2584.8	2038.6	1273.8
	1206.1	1195.6	2238.4	33722.3	51.58	
82	1.575	2975.8	2928.0	2550.7	2019.2	1275.3
	1209.9	1199.9	2237.7	33680.5	51.60	
83	1.625	2930.8	2884.3	2517.2	2000.3	1276.5
	1213.6	1203.8	2236.9	33640.3	51.62	
84	1.675	2883.1	2838.1	2481.8	1980.0	1277.6
	1217.1	1207.7	2236.2	33601.6	51.63	
85	1.725	2832.7	2789.1	2444.2	1958.4	1278.4
	1220.5	1211.4	2235.5	33564.5	51.65	
86	1.775	2781.7	2739.5	2406.1	1936.5	1279.0
	1223.6	1215.0	2234.8	33529.0	51.66	
87	1.825	2724.4	2683.8	2363.1	1911.6	1279.5
	1226.7	1218.4	2234.1	33495.1	51.67	
88	1.875	2664.0	2625.1	2317.9	1885.3	1279.7
	1229.5	1221.6	2233.4	33462.9	51.69	
89	1.925	2600.4	2563.3	2270.2	1857.5	1279.7
	1232.2	1224.7	2232.7	33432.4	51.70	
90	1.975	2552.0	2496.8	2218.9	1827.5	1279.5
	1234.7	1227.6	2232.0	33403.6	51.71	
91	2.025	2462.6	2429.3	2166.7	1796.9	1279.1
	1237.0	1230.4	2231.3	33376.5	51.73	
92	2.075	2369.2	2358.0	2111.5	1764.4	1278.5
	1239.2	1233.0	2230.5	33351.1	51.74	
93	2.125	2310.4	2281.4	2052.2	1729.5	1277.7
	1241.1	1235.4	2229.8	33327.4	51.75	
94	2.175	2251.3	2204.4	1992.6	1694.3	1276.6
	1242.9	1237.6	2229.1	33305.6	51.76	
95	2.225	2147.4	2122.9	1929.4	1656.9	1275.4
	1244.5	1239.6	2228.4	33285.5	51.77	
96	2.275	2061.0	2038.9	1864.3	1618.3	1274.0
	1245.9	1241.5	2227.7	33267.2	51.78	
97	2.325	1972.8	1953.2	1797.7	1578.8	1272.3
	1247.2	1243.2	2226.9	33250.7	51.79	
98	2.375	1883.5	1866.3	1730.3	1538.7	1270.4
	1248.2	1244.7	2226.2	33236.0	51.79	
99	2.425	1793.9	1779.2	1662.6	1498.3	1268.4
	1249.1	1246.0	2225.5	33223.1	51.80	
100	2.475	1704.8	1692.5	1595.2	1458.1	1266.1
	1249.7	1247.1	2224.8	33212.0	51.81	

EXIT PRESSURE

EXIT TEMPERATURE

113.5

1247.7

POWER PER UNIT LENGTH (KW/FT)

8.04

1. The maximum fuel temperature is 3569.4 F and occurs at $Z = 0.025$ ft. This compares to the 3548.2 F at the same location for normal core operation.
2. The maximum cladding temperature observed was 1279.7 F and occurred at $Z = 1.900$ ft. This compares to 1120.0 F at $Z = 1.925$ ft for normal operation.
3. The exit sodium temperature was 1247.7 F compared to 1100.0 F for normal operation.

5.6 Listing of Code

```
C
C
C
C-----VPI LMFBR THERMAL HYDRAULICS CODE.
C
C
C
      INTEGER M
      REAL KFU,KCL,KBC,M,NUCIFC,NU,MDOT,KCL1,KCL2,KFU1,KFU2
C
C      TEMPERATURE DEPENDENT PROPERTIES.
C
      KFU(T)=3.26743-0.24827E-2*T+0.69947E-6*T**2
      KCL(T)=0.65261E1+0.91565E-2*T-0.48934E-5*T**2+0.26882E-8*T**3-0.16
<793E-11*T**4+0.63502E-15*T**5
      KBC(T)=54.306-1.878E-2*T+2.0914E-6*T**2
      VIS(T)= 1.45675-0.14807E-2*T+0.5290E-6*T**2
      RHO(T)=59.566-7.95040E-3*T-0.2872E-6*T**2+0.06035E-9*T**3
      CP(T)=0.38935-1.10600E-4*T+3.4118E-8*T**2
C
C      SATURATION TEMPERATURE AS FUNCTION OF PRESSURE.
C
      TSAT(P)=0.75541E3+0.78670E2*ALOG(P)-0.30458E1*ALOG(P)**2+0.98415*
<LOG(P)**3
C
C      READING INPUT DATA.
C
      READ(5,5)DFU,DCL,S,HP,H
5  FORMAT(3F10.4,F10.2,F10.1)
      READ(5,10)GIN,TIN,PIN
10 FORMAT(E10.3,2F10.1)
      READ(5,15)OTPO,HE,OP
```

15 FORMAT(E10.3,F10.1,I10)

C
C
C

PRINTOUT OF INPUT DATA.

WRITE(6,20)

20 FORMAT(1H1,1X,'*****',/3X,'L
<MFR THERMAL HYDRAULICS CODE',/2X,'*****'
<*',//,3X,'INPUT DATA',//)

WRITE(6,25)DFU,DCL,S,H,HD

25 FORMAT(3X,'FUEL O.D.',6X,'CLAD O.D.',6X,'ROD PITCH',6X,'ACTIVE COR
<E LENGTH',6X,'WIRE WRAP PITCH',/3X,'(INCH)',7X,'(INCH)',7X,'
<(INCH)',12X,'(INCH)',14X,'(INCH)',/4X,F6.4,9X,F6.4,9X,F6.4,
<14X,F6.2,16X,F6.2,/))

WRITE(6,30)GIN,TIN,PIIN

30 FORMAT(3X,'INLET MASS VELOCITY',3X,'CORE INLET TEMPERATURE',3X,'CO
<RE INLET PRESSURE',/5X,'(LB/HR-FT**2)',13X,'(F)',16X,'(PSI
<A)',/7X,E11.4,14X,F7.2,17X,F7.2,/))

WRITE(6,35)QTPD,HE

35 FORMAT(3X,'VOLUMETRIC THERMAL',4X,'EXTRAPOLATED HEIGHT',/4X,'SOUR
<CE STRENGTH',/4X,'(BTU/HR-FT**3)',11X,'(INCH)',/6X,E11.4,14X,
<F6.2,//))

WRITE(6,40)OP

40 FORMAT(19X,'OPTION',3X,I2,///,3X,'E N D O F I N P U T D A T A',
</,3X,'*****',//))

C
C
C

CONVERTING INCHES TO FEET.

DFU=DFU/12.0

S=S/12.0

DCL=DCL/12.0

H=H/12.0

HE=HE/12.0

C
C
C
HP = HP/12.0

PI=3.14159

C
C
C
GEOMETRY CALCULATIONS.

DW = S-DCL

AFL=S**2*COS(PI/6.0)/2.- PI/8.0*(DCL**2 + DW**2)

PW=PI*(DCL+DW)/2.

DEQ=4.0*AFL/PW

DR=DW/DEQ

SRAT=S/DCL

C
C
C
C
RATIO OF FRICTION FACTOR IN SMOOTH TRIANGULAR COOLANT CHANNEL
TO CIRCULAR TUBE FRICTION FACTOR.

FRAT=-3.4751+8.0528*SRAT-4.7047*SRAT**2+0.91521*SRAT**3

C
C
C
C
CALCULATION OF RATIO OF FRICTION FACTOR IN WIRE-WRAPPED COOLANT
CHANNEL TO THAT IN SMOOTH TRIANGULAR CHANNEL.

Y= 0.18598-0.13640E1*DR+0.28944E1*DR**2

FWM=1.195-Y*(HP-.75)/.25

C
C
C
MASS FLOW RATE CALCULATION.

MDOT=GIN*AFL

C
C
C
SELECTION OF AXIAL CALCULATION INCREMENT.

DELL=H/100.0

C
C
CALCULATION OF PRESSURE LOSS AT INLET OF CORE.

C
UB=GIN/RHO(TIN)/3600.0
RE=UB*DEQ*RHO(TIN)/VIS(TIN)*3600.0
FCIRC=0.184/RE**0.2
F=FCIRC*FRAT*FWWM
DELPE=F*DELL*RHO(TIN)*UB**2/DEQ/2.0/32.2*23.0
DELPE=0.5*RHO(TIN)*UB**2/2.0/32.2
WRITE(6,42)

42 FORMAT(5X,'AT THE INLET OF THE COFF',//)

WRITE(6,45)UB,RE,FCIRC

45 FORMAT(3X,'CHANNEL AVE. VELOCITY ',2X,'REYNOLDS #',3X,'FRICTION FA
<CTOR',/,7X,'(FT/SEC)',/,8X,F6.2,12X,F8.1,8X,F7.4,//)

WRITE(6,50)

50 FORMAT('*****
<*****
<',//)

C
C
C
CALCULATION OF CONDITIONS AT BEGINNING OF FIRST INCREMENT.

PI=PIN-(DELPE+DELPE)/144.0

TBI=TIN

I=1

C
C
C
CALCULATION OF AXIAL COORDINATE OF CENTER OF FIRST INCREMENT.

ZC=-H/2.0+DELL/2.0

C
C
C
PRINT OUT OF COLUMN HEADINGS.

WRITE(6,55)

55 FORMAT(2X,'NO',4X,'7-LCC.',6X,'TO',7X,'T1/4',6X,'T1/2',6X,'T3/4',7
<X,'TF',6X,'T CLAD',4X,'T BULK',4X,'T SAT',3X,'H T COEF',4X,'DELTA

<P',//)

C
C CALCULATION OF AVERAGE BULK TEMPERATURE FOR INCREMENT.
C

60 QTPAV=QTPD*COS(PI*ZC/HE)

 TB2=TB1+QTPAV*PI*DFU**2.0*DELL/4.0/MDOT/CP(TB1)/2.0

C
C THE DIVISION BY 2 IN THE PREVIOUS CALCULATION IS PEQUIRED BE -
C CAUSE ONLY HALF OF THE ENERGY GENERATED IN THE FUEL ROD ENTERS
C THE CHANNEL.
C

 TBAV=(TB1+TB2)/2.0

C
C CALCULATION OF PRESSURE DROP AND AVERAGE PRESSURE FOR INCREMENT
C

 UB=GIN/RHO(TBAV)/3600.0

 F=UB*DEQ*RHO(TBAV)/VIS(TBAV)*3600.0

 FCIRC=0.184/RE**0.2

 F=FCIRC*FRAT*FWWM

 DELPE=F*DELL*RHO(TBAV)*UB**2.0/DEQ/2.0/32.2

 P2=P1-DELPE/144.0

 PAV=(P1+P2)/2.0*144.0

C
C CALCULATION OF AVERAGE SATURATION TEMPERATURE FOR INCREMENT.
C

 TSATAV=TSAT(PAV)

C
C CALCULATION OF HEAT TRANSFER COEFFICIENT FOR INCREMENT.
C

 PR=CP(TBAV)*VIS(TBAV)/KRC(TBAV)

 PE=RE*PR

 NU=-88.0+130.8*SRAT-41.67*SRAT**2

```

PEQ=336.)*SRAT-110.0
IF(PE-PEQ)70,70,65
65 NU=NU+0.025*(PE-PEQ)**0.8
70 HTC=NU*KBC(TBAV)/DEQ

```

```

C
C     CALCULATION OF TEMPERATURE AT OUTSIDE SURFACE OF CLADDING FOR
C     INCREMENT.
C

```

```

TSAV=TBAV+QTPAV*DFU**2.0/4.0/DCL/HTC

```

```

C
C     CHECK FOR POSSIBILITY OF SURFACE BOILING. IF DETECTED, "SUR-
C     FACE BOILING" PRINTED OUT AND CALCULATIONS TERMINATED.
C

```

```

IF(TSAV-TSATAV)95,75,75
75 WRITE(6,90)
80 FORMAT(/,10X,' SURFACE BOILING',/)
WRITE(6,85)
85 FORMAT(/,10X,' SURFACE TEMPERATURE',10X,' SATURATION TEMPERATURE',/)
WRITE(6,90) TSAV,TSATAV
90 FORMAT(16X,F9.2,10X,F9.2)
GO TO 160

```

```

C
C     CALCULATION OF TEMPERATURE AT OUTSIDE SURFACE OF FUEL FOR IN-
C     CREMENT. DETERMINED BY ADDING TEMPERATURE RISE ACROSS CLADDING
C     TO TEMPERATURE AT OUTSIDE SURFACE OF CLADDING. AN ITERATION
C     TECHNIQUE IS USED TO OBTAIN THE CLADDING THERMAL CONDUCTIVITY
C     TO WITHIN 1%.
C

```

```

95 KCL1=KCL(TSAV)
100 TF=TSAV+QTPAV*DFU**2.0/8.0/KCL1*ALOG(DCL/DFU)
TCLAV=(TSAV+TF)/2.0
KCL2=KCL(TCLAV)

```

```
FRR=ABS((KCL1-KCL2)/KCL2)
```

```
IF (ERR-0.001) 110, 110, 105
```

```
105 KCL1=KCL2
```

```
GO TO 100
```

```
C  
C  
C     CALCULATION OF TEMPERATURE AT CENTER OF FUEL FOR INCREMENT. AN  
C     ITERATION TECHNIQUE IS USED TO OBTAIN FUEL THERMAL CONDUCTIVITY  
C     WITHIN 1%.  
C
```

```
110 KFU1=KFU(TF)
```

```
115 TO=TF+QTPAV*DFU**2.0/16.0/KFU1
```

```
TFAV=(TF+TO)/2.0
```

```
KFU2=KFU(TFAV)
```

```
ERR=ABS((KFU1-KFU2)/2.0)
```

```
IF (ERR-0.001) 125, 125, 120
```

```
120 KFU1=KFU2
```

```
GO TO 115
```

```
C  
C  
C     CALCULATION OF FUEL TEMPERATURE AT 1/4, 1/2, AND 3/4 FUEL RADII  
C     FOR INCREMENT.  
C
```

```
125 T14=TO-QTPAV*DFU**2.2/16.0/KFU1/16.0
```

```
T12=TO-QTPAV*DFU**2.0/16.0/KFU1/4.0
```

```
T34=TO-QTPAV*DFU**2.0/16.0/KFU1/16.0*9.0
```

```
C  
C  
C     PRINTOUT OF RESULT FOR CALCULATION INCREMENT.
```

```
*WRITE(6,130)I,ZC,TO,T14,T12,T34,TF,TSAV,TBAV,TSATAV,HTC,DELPH
```

```
130 FORMAT(1X,I3,F10.3,9F10.1,4X,F6.2)
```

```
C  
C  
C     CHECK TO SEE IF CALCULATIONS HAVE BEEN COMPLETED FOR ENTIRE  
C     CORE.  
C
```

```

C
IF(I-100)135,140,140
C
C   SETTING CONDITIONS FOR BEGINNING OF NEXT CALCULATION INCREMENT.
C
135 I=I+1
    ZC=ZC+DELL
    TB1=TB2
    P1=P2
C
C   TRANSFERRING TO START CALCULATIONS FOR NEXT INCREMENT.
C
GO TO 60
C
C   CALCULATION OF CORE EXIT CONDITIONS OF COOLANT.
C
140 UB=GIN/RHO(TB2)/3600.0
    RE=UB*DEQ*RHO(TB2)/VIS(TB2)*3600.0
    FCIRC=0.184/RE**0.2
    F=FCIRC*FRAT*FWM
    DELPF=F*DELL*RHO(TB2)*UB**2/DEQ/2.0/32.2*103.0
    DELPE=RHO(TB2)*UB**2/2.0/32.2
C
C   CALCULATION OF CORE EXIT CONDITIONS OF COOLANTS .
C
PEX=P2-(DELPF+DELPE)/144.0
TEX=TB2
C
C   PRINTOUT OF CORE EXIT COOLANT CONDITIONS.
C
WRITE(6,145)
145 FORMAT(/,10X,'EXIT PRESSURE',10X,'EXIT TEMPERATURE',/)

```

```
WRITE(6,150)PEX,TEX  
15) FORMAT(13X,F6.1,18X,F6.1)
```

```
C  
C  
C  
C  
CALCULATION OF AVERAGE POWER OF FUEL ROD IN KW/FT.  
PRINTOUT OF AVERAGE POWER.
```

```
POVL=QTPG*HE*CFU**2/2.0*SIN(PI*H/2.0/HE)/H
```

```
POVL=POVL/3412
```

```
WRITE(6,155)POVL
```

```
155 FORMAT(//,5X,' POWER PER UNIT LENGTH (KW/FT) ',F15.2,//////)
```

```
160 STOP
```

```
END
```

- 83 -

6.0 References

1. Glasstone, S., and M. C. Edlund, The Elements of Nuclear Reactor Theory, D. Van Nostrand Co., Inc., Princeton, N.J., 1952.
2. Zwiefel, P. F., Reactor Physics, McGraw Hill Book Company, New York N.Y., 1973.
3. Glasstone, S., and A. Sesonke, Nuclear Reactor Engineering, D. Van Nostrand Co., Inc., Princeton, N.J., 1963.
4. El-Wakil, M. M., Nuclear Heat Transport, International Textbook Company, Scranton, Pa., 1971.
5. Holman, J. P., Heat Transfer, Third Edition, McGraw-Hill Book Company New York, N.Y., 1972.
6. Kreith, F., Principles of Heat Transfer, Third Edition, Intext Educational Publishers, New York, N.Y., 1973.
7. Shames, I. H., Mechanics of Fluids, McGraw Hill Book Company, New York, N.Y., 1962.
8. Sabersky, R. H., and A. J. Acosta, Fluid Flow, The Macmillan Co., New York, N.Y., 1964.
9. Baumeister, T., and L. S. Marks, Standard Handbook for Mechanical Engineers, McGraw-Hill Book Co., New York, N.Y., 1967.
10. Flow of Fluids Through Valves, Fittings, and Pipe, Technical Paper No. 410, Crane Co., Chicago, Illinois, 1965.
11. Deissler, R. G., and M. F. Taylor, "Reactor Heat Transfer Conference," New York, TID-7529, Pt. 1, Book 1, November, 1957, pp. 416-461.
12. Reihman, T. C., "An Experimental Study of Pressure Drop in Wire-wrapped FFTF Fuel Assemblies," BNWL-1207 FF, September, 1969.
13. Lyon, R. N., Ed., Liquid Metals Handbook, Third Edition, Washington, D.C.: Atomic Energy Commission and Department of the Navy, 1952.
14. Lubarsky, B., and S. J. Kaufman, "Review of Experimental Investigations of Liquid-Metal Heat Transfer, NACA Report 1270, 1956.
15. Deissler, R. G., "Analysis of Fully Developed Turbulent Heat Transfer at Low Peclet Numbers in Smooth Tubes with Application to Liquid Metals," NACA RM E52F05, August, 1952.
16. Martinelli, R. C., "Heat Transfer in Molten Metals," Trans. ASME, Vol. 69, No. 8, 1947, pp. 947-960.

17. Borishansky, V. M., and E. V. Firsova, "Heat Exchange in the Longitudinal Flow of Metallic Sodium Past a Tube Bank," *At. Energ.*, Vol. 14, 1963, p. 584.
18. Subbotin, V. I., P. A. Ushakov, and P. L. Kirillov, "Heat Removal From Reactor Fuel Elements Cooled by Liquid Metals," Paper No. 328, Third United Nation's International Conference on the Peaceful Uses of Atomic Energy, Geneva, August 31-Sept. 9, 1964.
19. Dwyer, O. E., "Analytical Study of Heat Transfer to Liquid Metals Flowing In-Line Through Closely Packed Rod Bundles", *Nuclear Science and Engineering*, Vol. 25, No. 4, August, 1966, pp. 343-358.

7.0 Problems

1. By performing an energy balance on a differential element with sides dx , dy , and dz , derive the steady state heat conduction equation in Cartesian coordinates.
2. Derive the steady state heat conduction equation in cylindrical coordinates.
3. Develop an expression for the temperature distribution in a long, thin, hollow cylindrical fuel element with inner radius r_i , outer radius r_o , and volumetric thermal source strength q''' . Assume that the inner surface is insulated and at temperature T_i .
4. A long, thin, hollow cylindrical fuel element with volumetric thermal source strength q''' is cooled on both the inner and outer surfaces ($r = r_i$ and $r = r_o$ surfaces) such that the surface temperatures are T_i and T_o , respectively. Derive an expression for the location of the maximum radial temperature in the fuel.
5. Calculate the ratio of peak power to average power for a fuel rod of constant cross section assuming that the volumetric thermal source strength varies as $q''' = q'''_0 \cos(\pi Z/H_c)$ and that the extrapolation length is 10% of the core height. Compare this ratio to that for the case where the extrapolation length is assumed to be zero.
6. Show that for a cylindrical shell without internal heat generation the use of an average constant thermal conductivity evaluated at the arithmetic mean of the inner and outer surface temperatures is equivalent to a linear variation of thermal conductivity with temperature.
7. A LMFBR fuel rod consists of 0.250 in. diameter UO_2 - PuO_2 fuel pellets in a 0.250 in. ID, 0.300 in. OD tube of stainless steel cladding. The heat transfer coefficient at the outer surface of the fuel rod is 30,000 Btu/hr-ft²-F. The thermal conductivities of the fuel and cladding are 1.95 Btu/hr-ft-F and 12.8 Btu/hr-ft-F, respectively. The coolant bulk temperature is 900 F and the volumetric thermal source strength is 1.8×10^8 Btu/hr-ft³. Determine the maximum fuel temperature and the maximum cladding temperature.
8. Same as Problem 7 except the ID of the cladding is 0.270 in. The 0.020 in. diametral gap between the fuel and cladding is filled with helium gas. Assuming that the heat transfer through the helium is by molecular conduction only ($k_{he} = 0.140$ Btu/hr-ft-F) determine the maximum fuel and cladding temperatures.
9. A four foot long LMFBR fuel assembly contains 0.260 in. OD fuel rods spaced 0.320 in. in a triangular array. The wire wrap helical pitch is 9 inches. The average conditions in the core are 150 psia and 950 F. The mass velocity of the liquid sodium is 5.0×10^6 lbm/hr-ft². Determine the pressure drop through the core.

10. Determine the effect on pressure drop of a 10% increase in cladding OD for the fuel in Problem 9. Assume the spacing, coolant conditions and mass velocity remain the same. (Note the wire wrap diameter must be reduced by 0.026 in. to maintain the same spacing of the fuel rods).
11. Determine the heat transfer coefficient for the fuel and flow conditions of Problem 9.
12. A LMFBR fuel consists of 0.250 in. diameter $\text{UO}_2\text{-PuO}_2$ fuel pellets contained in 0.250 in. ID, 0.285 in. OD type 347 stainless steel cladding. The fuel rods are spaced 0.350 in. in a triangular array. At a particular location in the core the pressure is 100 psia, the liquid sodium temperature is 1000 F and the coolant velocity is 24 ft/sec. The volumetric thermal source strength is 1×10^8 Btu/hr-ft². Determine the heat transfer coefficient.
13. Determine the coolant velocity required to keep the temperature rise across the convective layer below 12 F for the fuel and coolant conditions of Problem 12.
14. In a nuclear fuel rod the volumetric thermal source strength varies axially as $q'''(z) = q_o''' \cos(\pi z/H)$. The energy generated in this rod is removed by coolant channels which have a combined mass flow rate of \dot{m} and an inlet temperature of T_{in} . Designate the fuel diameter as D_f and the cladding OD as D_s . Develop an expression for the axial variation of the temperature at the inside surface of the cladding. Your expression should contain only T_{in} , q_o''' , D_f , D_s , H , H_e , \dot{m} , C_p , h , k_c , and Z .
15. From the expression developed in Problem 14 determine the location of the maximum cladding temperature in the reactor.
16. Determine the location of the maximum fuel temperature for the fuel rod-coolant channel system of Problem 14.
17. A 1400 Mw(t) liquid sodium cooled LMFBR contains 25,000 fuel rods each composed of 0.200 in. diameter $\text{UO}_2\text{-PuO}_2$ fuel pellets in 0.230 in OD tubes of type 347 stainless steel cladding. The fuel rods are spaced 0.290 in. in a triangular array. The reactor core height is 60 in. The coolant inlet conditions are 250 psia, 700 F and the average mass velocity is 5.4×10^6 lbm/hr-ft². The thermal source strength varies as $q''' = q_o''' \cos(\pi z/H)$ and $H_e = 65$ in. Determine the maximum fuel temperature and the maximum cladding temperature in the core.
18. Determine the % reduction in coolant flow that will cause the maximum cladding temperature to approach the allowable limit of 1250 F for the reactor described in Problem 17.
19. Determine the % overpower that the reactor described in Problem 17 can produce without exceeding the 1250 F maximum cladding temperature limit. What is the coolant temperature at the core exit for this limiting case?

20. A 1200 Mw(t) liquid sodium cooled LMFBR contains 30,000 fuel rods with an active fuel length of 53 in. Each fuel rod consists of 0.180 in. diameter $\text{UO}_2\text{-PuO}_2$ pellets enclosed in 0.210 in. OD type 347 stainless steel cladding. The fuel rods are spaced 0.260 in. in a triangular array. The inlet coolant conditions are 700 F, 250 psia and the average velocity in the core is 32 ft/sec. The axial power distribution is a truncated cosine function. Assume an extrapolation length of 3 in. Determine the location and magnitude of the maximum fuel, cladding, and coolant temperature.
21. Determine the % of overpower that would result in a 1200 F maximum allowable cladding temperature limit being exceeded for the core described in Problem 20. At what axial location does this 1200 F temperature occur?